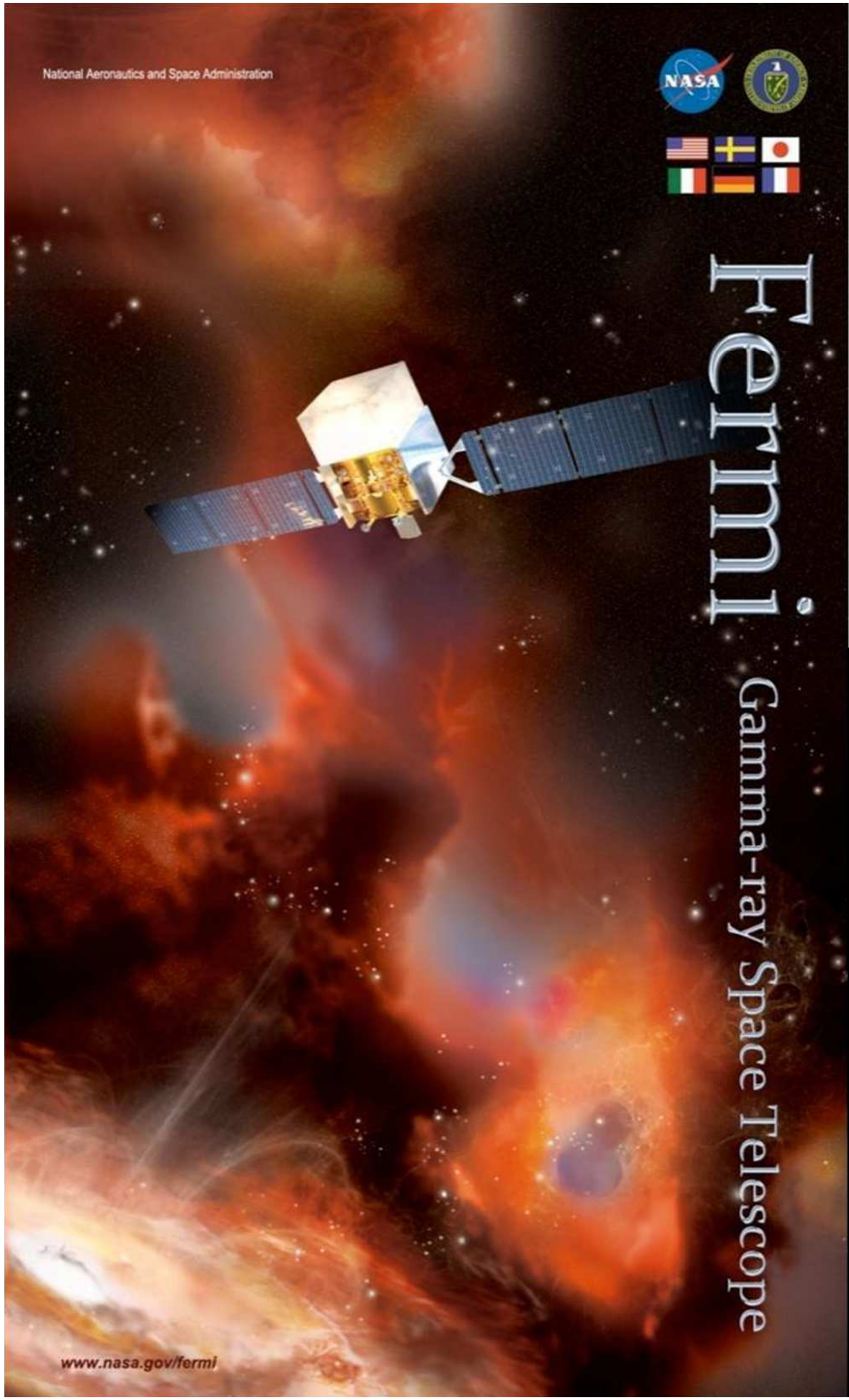

AGNs with the Fermi-LAT

Benoît Lott
CEN Bordeaux-Gradignan, France
lott@cenbg.in2p3.fr

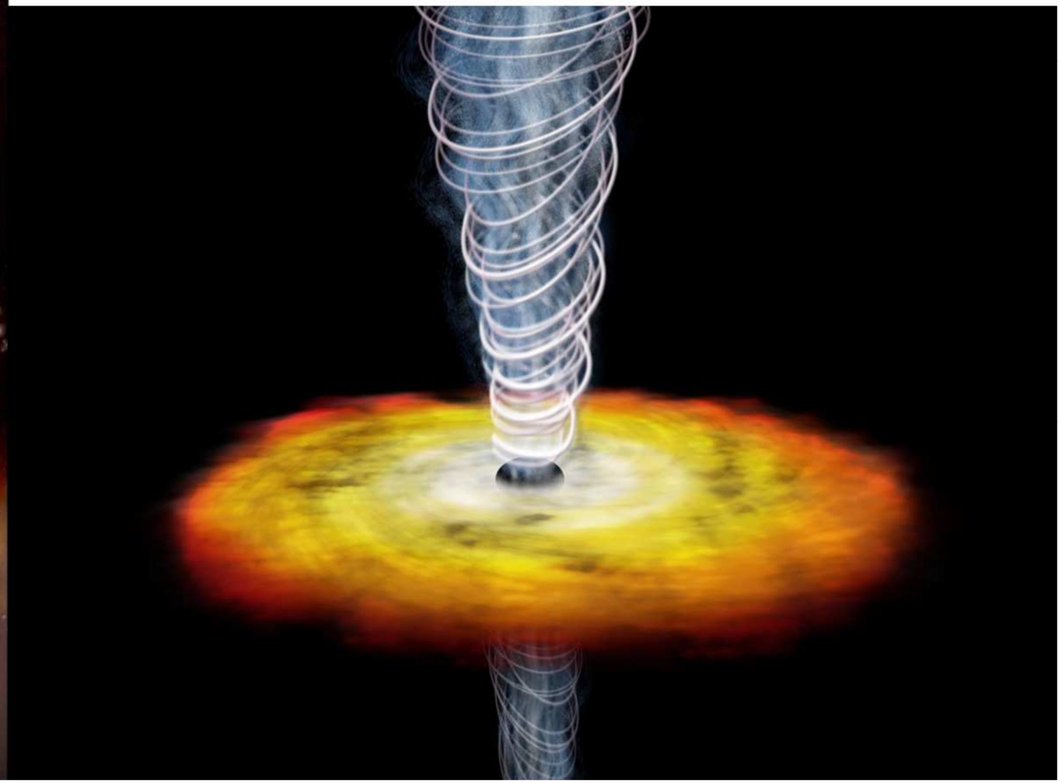

EGRET legacy

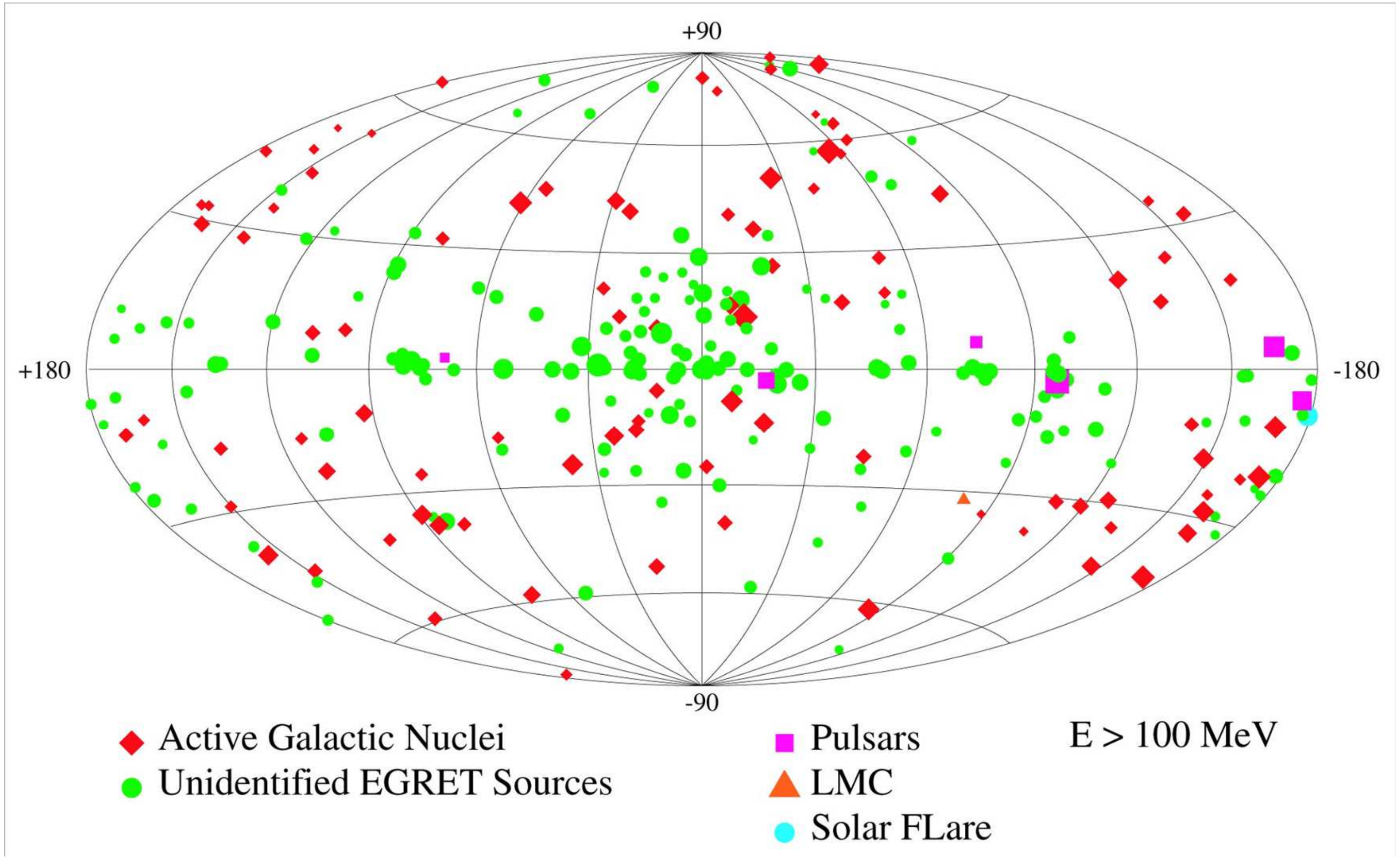

70 high-confidence blazars: 56 FSRQs, 14 BL Lacs

3C 454.3 lightcurve

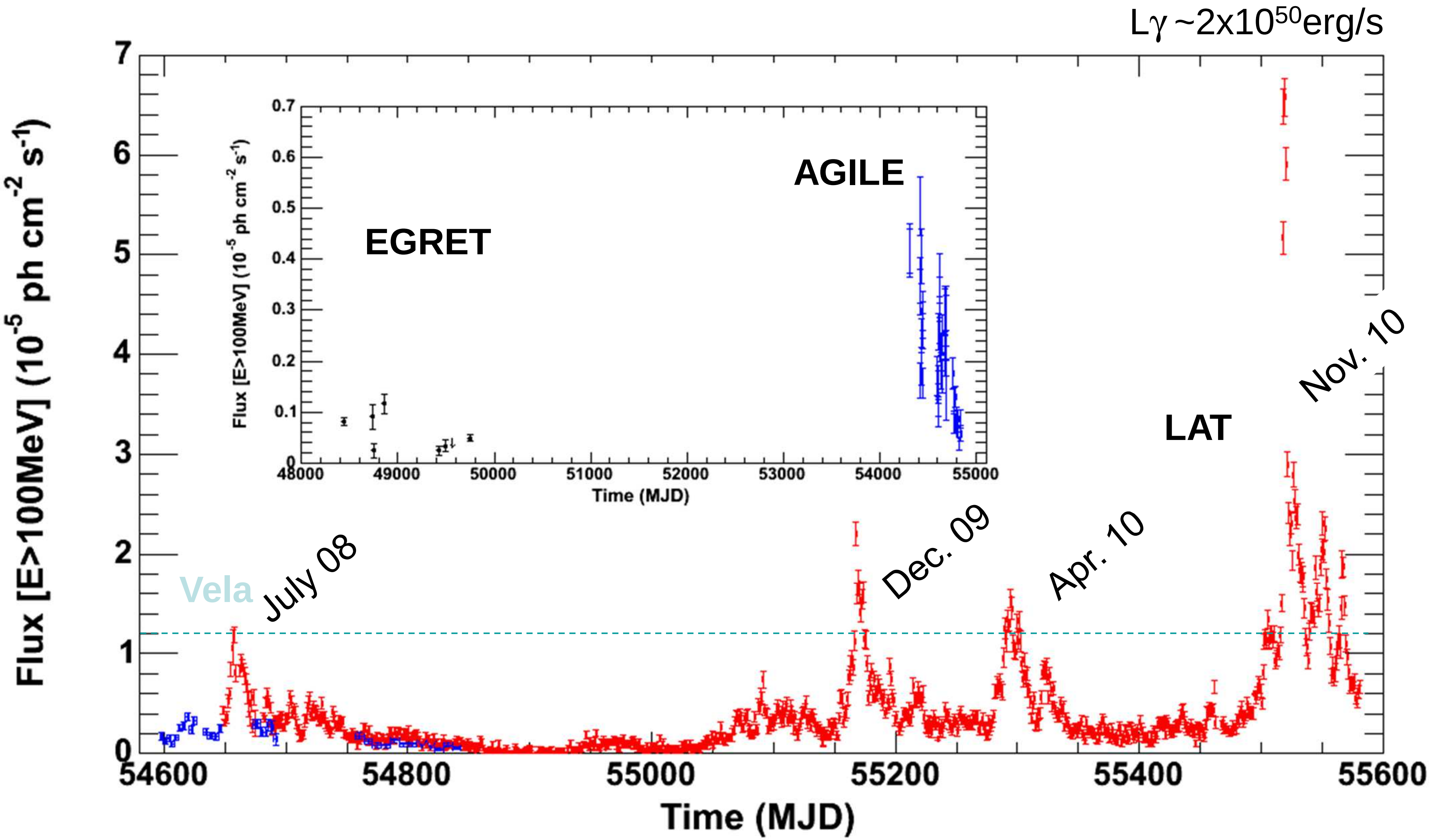

Active Galactic Nuclei: generalities

Radio galaxies

5-15% of active galaxies
(others are mostly Seyferts)
Mostly of the elliptical type (Seyferts : spirals)
Galaxies displaying extended radio lobes
(up to 10 x larger than the galaxy)

2 classes

- **Fanaroff-Riley 1:** large opening angle, brighter close to the core, low luminosity, close
- **Fanaroff-Riley 2:** highly collimated jet, lobe brightened with hot spots, luminous, distant

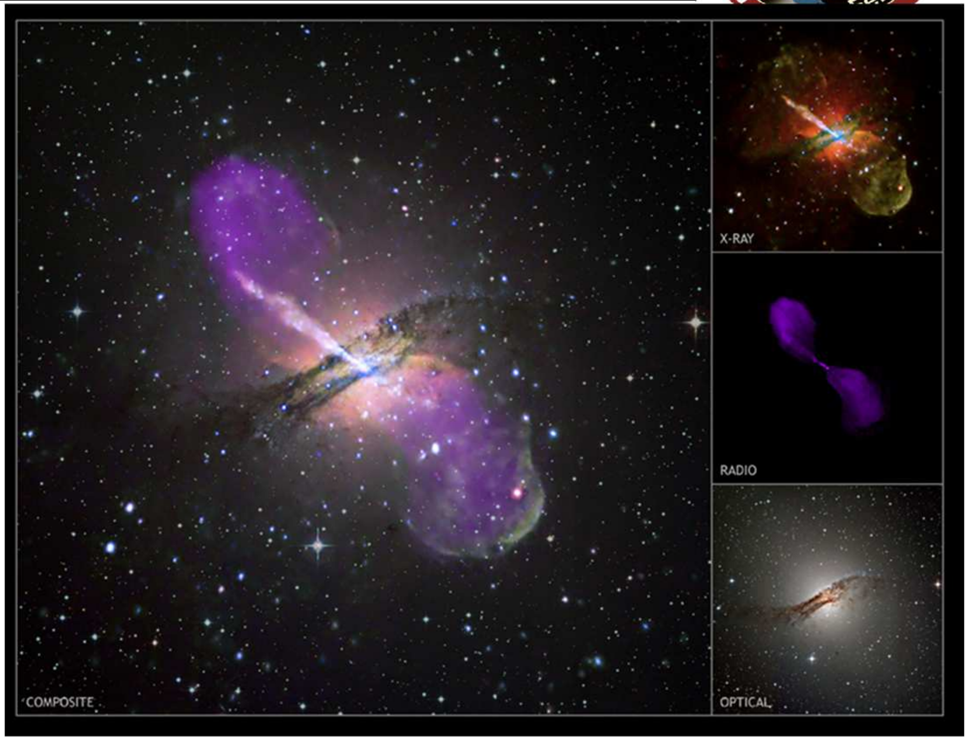

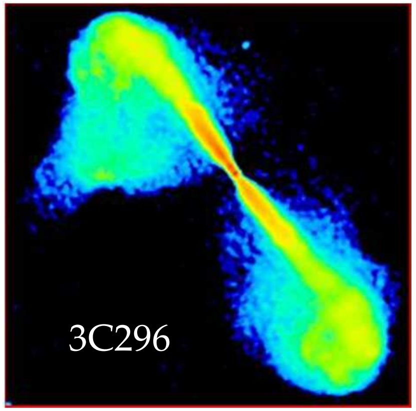

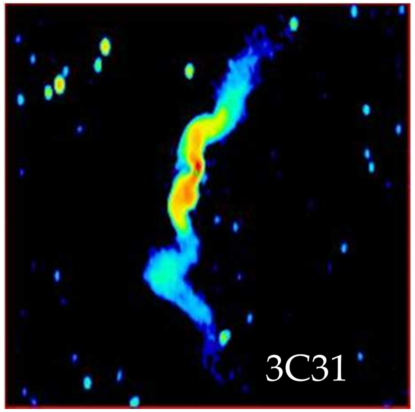

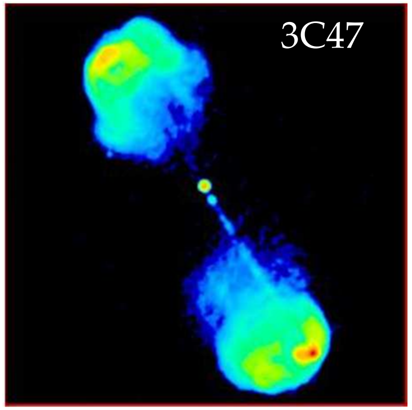

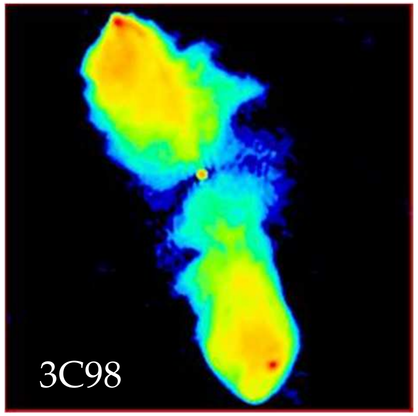

The jet

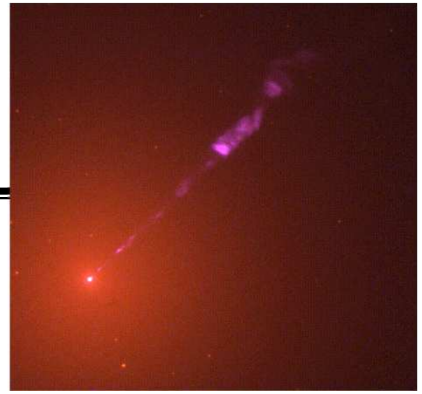

- **Origin:**
  - **disk accretion (Blandford-Payne)?**
  - **black-hole spin (Blandford-Znajek)?**
- **Collimated by magnetic field/external pressure**
- **Opening angle ~1/Γ**
  Γ = bulk Lorentz factor~10
- **Composition?**
  - **Poynting flux in the inner part to avoid Compton drag?**
  - **matter (plasma) dominates at larger distance**
  - **normal (e^-p^+) or electron (e^-e^+) plasma?**
- **Total power is**
  $P=\pi R^2\Gamma^2 c(U'_B+U'_{rad}+U'_e+U'_p)$
  U' : energy density in comoving frame

1.) Mass Accretion onto Black Hole

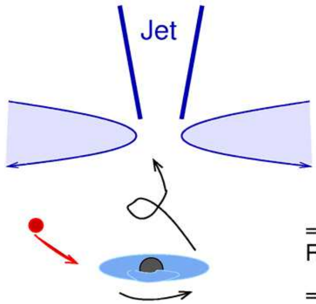

=> Extraction of up to 42.6% of Rest Mass Energy of Infalling Material

=> Accretion Disk => Jet Matter

2.) Extraction of Rotational Energy of Black Hole

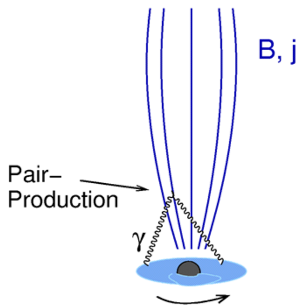

=> Extraction of up to 29% of Rest Mass Energy of Black Hole

=> Electron/Positron Jet

=> Different Jet Matter
Different AGN Life Time

P. Coppi

Unification scheme

Powered by accretion onto a central, supermassive black hole $10^{8\text{-}9}\ M_\odot$

Inner part of the disk shines very brightly: *quasar* phenomenon

Observed properties governed by angle w.r.t. line of sight

1 pc = 3×10^{16} m

$r_S=10^{-5}\ (M/10^8\ M_\odot)$ pc

Disk size: 10^{-3} pc

Base of VLBI jet: 1-10 pc

Broad-Line Region (BLR): 0.01-0.1 pc

Narrow-Line Region (NLR): 100-1000 pc

Tore: 100 pc

Galaxy diameter: 100 kpc

Radio lobes: 1 Mpc

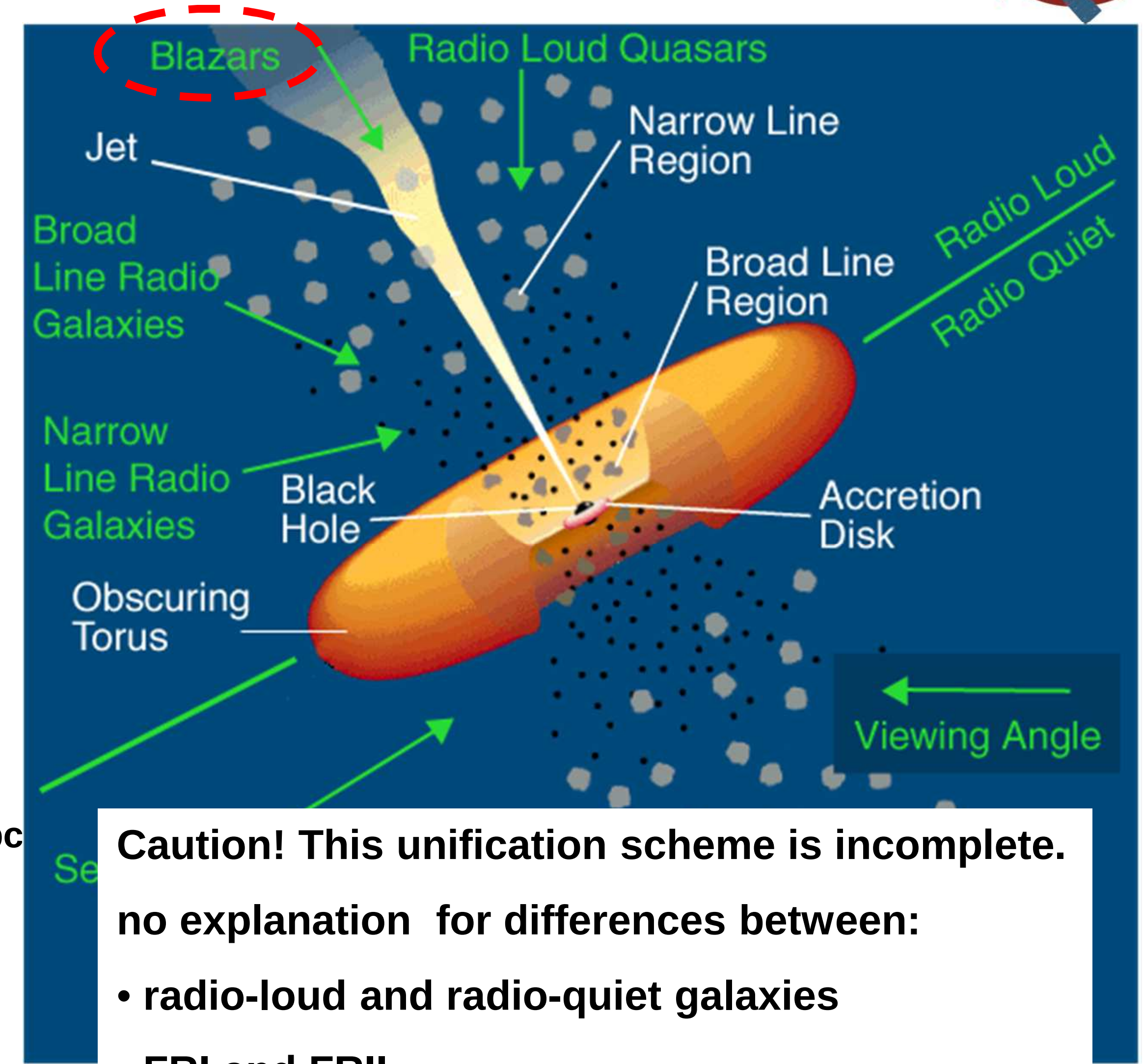

Caution! This unification scheme is incomplete.

no explanation for differences between:

- **radio-loud and radio-quiet galaxies**
- **FRI and FRII**

Blazar basics

Blazars

Jet directed close to line-of-sight
- **large apparent luminosity**
- **rapid variability**
- **“core dominated” in radio**
- **high optical polarisation**
- **large radio brightness**
- **superluminal motion**

Relativistic aberrations!

Doppler factor:

$$\delta = \frac{1}{\Gamma(1-\beta\cos\theta)}$$

For $\theta=0$, $\delta=2\Gamma$

For $\theta=1/\Gamma$, $\delta\sim\Gamma$

$\delta\cong 10\text{–}50$

$$\Delta t_{obs} = \delta^{-1}\Delta t'$$

$$\nu = \delta\nu'$$

$$I(\nu) = \delta^3 I'(\nu')$$

$$I = \delta^4 I'$$

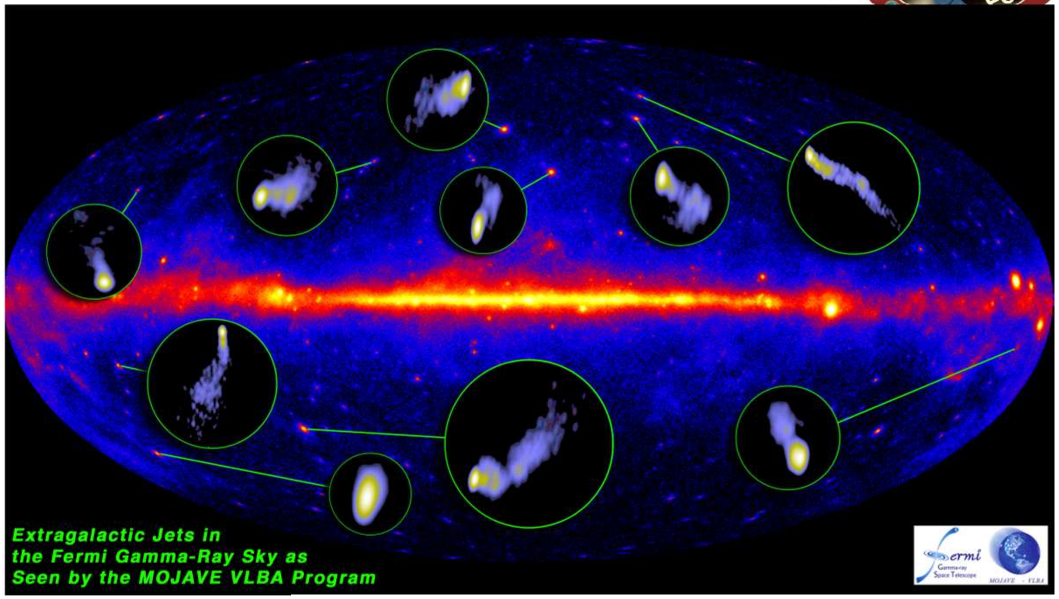

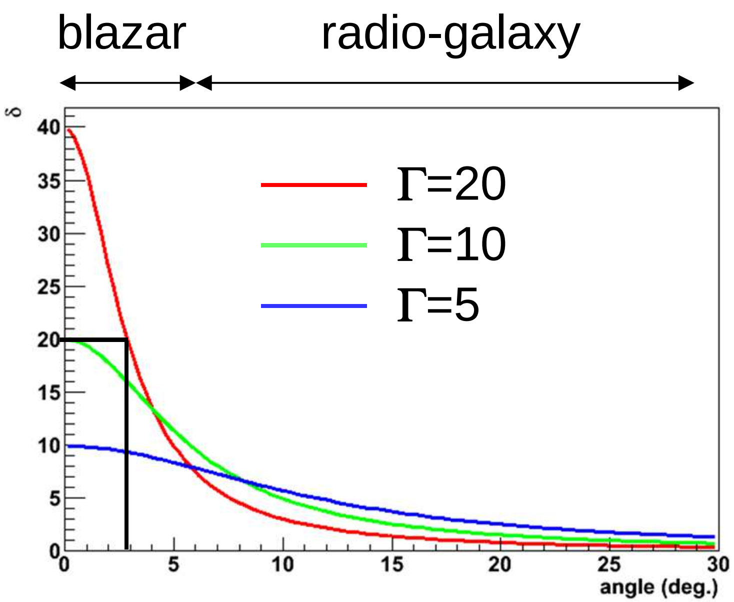

Constrains on β come from superluminal motions, and γ–γ opacity arguments (δ)

Blazar classes

FSRQ: Flat Spectrum Radio Quasar
BL Lac: named after prototype BL Lacertae

class	FSRQs	BLLacs
Defining property	strong emission lines	nearly lineless
Environment		
Power		
Parent population		
Synchrotron hump in SED		
Redshift		

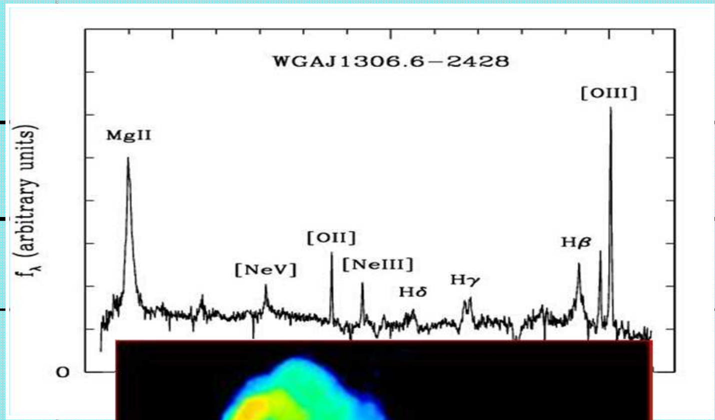

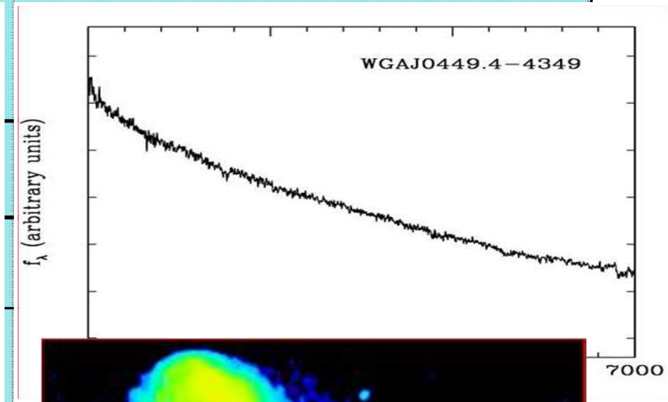

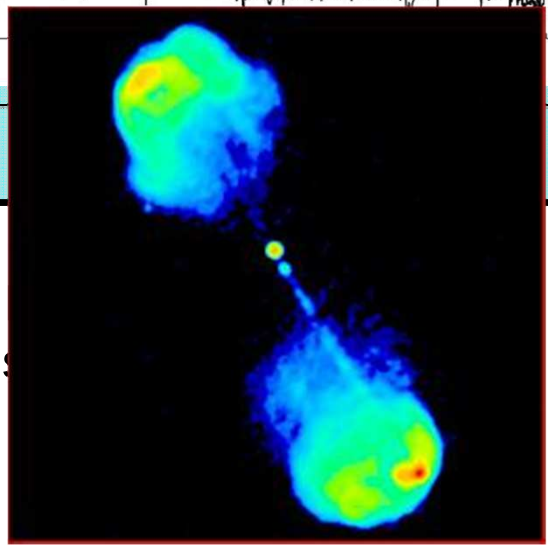

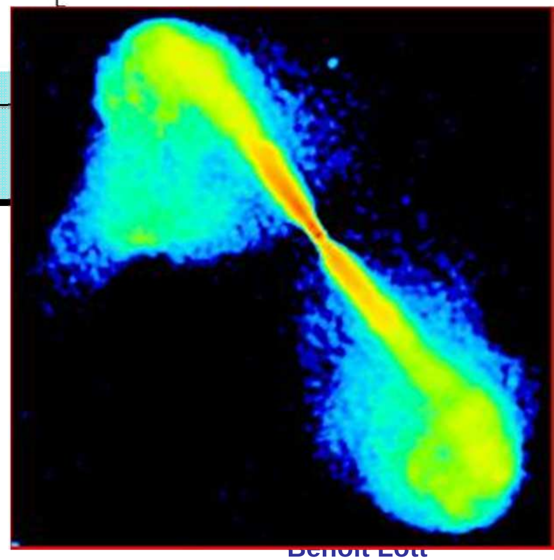

BL Lacs redshifts are
Many redshifts are mi

Blazar Spectral Energy Distributions (SEDs)

" two-hump" SEDs in νFν

Low-energy peak: ***Synchrotron***

- **Low-spectrum peaked (LSP/LBL) IR-optical ($\nu_{syn}<10^{14}$Hz)**
- **Intermediate-spectrum peaked (ISP-IBL) : UV ($10^{14}<\nu_{syn}<10^{15}$Hz)**
- **High-spectrum peaked (HSP-HBL) : X-rays ($\nu_{syn}>10^{15}$Hz)**

High-energy peak:

- **leptonic models:** ***Inverse Compton*** **upscattering of seed photons**
  - **synchrotron: "*Synchrotron Self Compton*"**
  - **External to the jet: *"External Compton*" (disk, BLR, torus)**
- **Hadronic models:** ***photoproduction, synchrotron…***

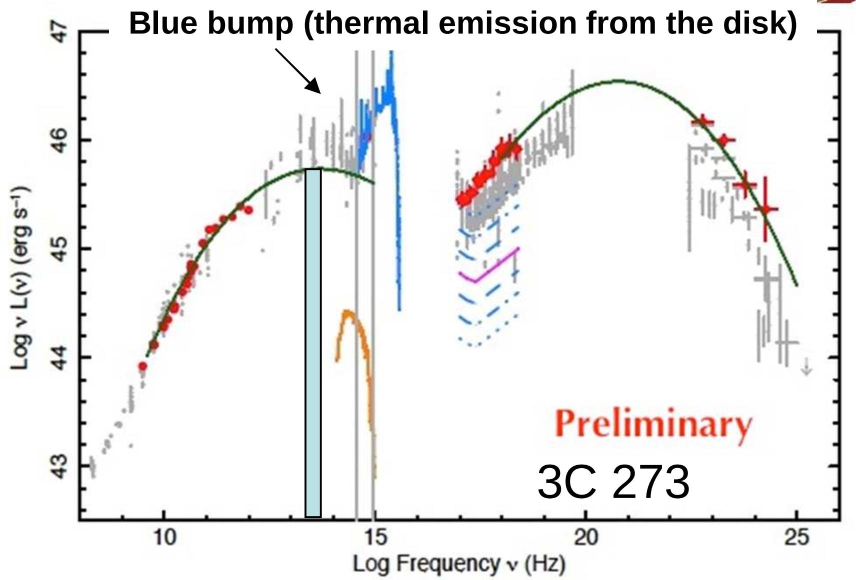

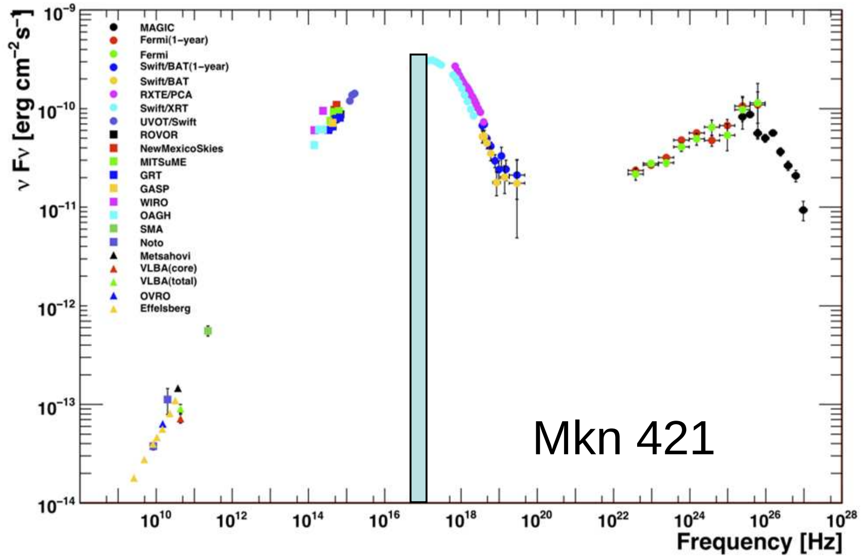

Gamma-ray Blazar/AGN populations

Association-Classification

Two associations methods:
Bayesian method
Likelihood ratio (LR) method
Two classification schemes:
• Optically-based (stength of broad lines): FSRQs, BL Lacs, BCUs (aka Sources of Unknown Type)
• SED-based: Low-, Intermediate-, High-Synchrotron-Peaked sources (LSPs, ISPs, HSPs resp.)
3LAC: manually-controled SED fit

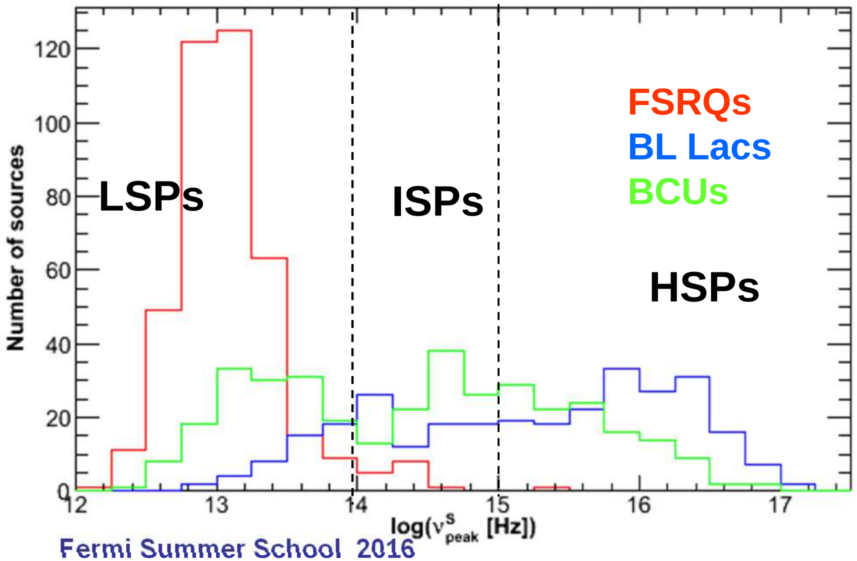

Catalogs used for association

- Véron-Cetty & Véron
- BZCAT
- VLBA Calibrator list
- CRATES
- CGRaBs
- TeVCat
- ATCA 20-GHz survey
- WISE gamma-ray blazar candidates
- 1WHSP
- NRAO VLA Sky Survey
- Sydney University Mongolo Sky Survey
- ROSAT All Sky Survey Bright and Faint Source Catalogs

False-positive rate <2%

The Third LAT AGN catalog (3LAC)

Ackermann M. et al., 2015, ApJ, 810, 14

- **48 month data set**
- **2192 TS>25, |b|>10° sources**
- **3LAC: 1591 counterparts**
  1563 sources
- **1444 AGNs in *Clean Sample*** **(no dup., no flags)**

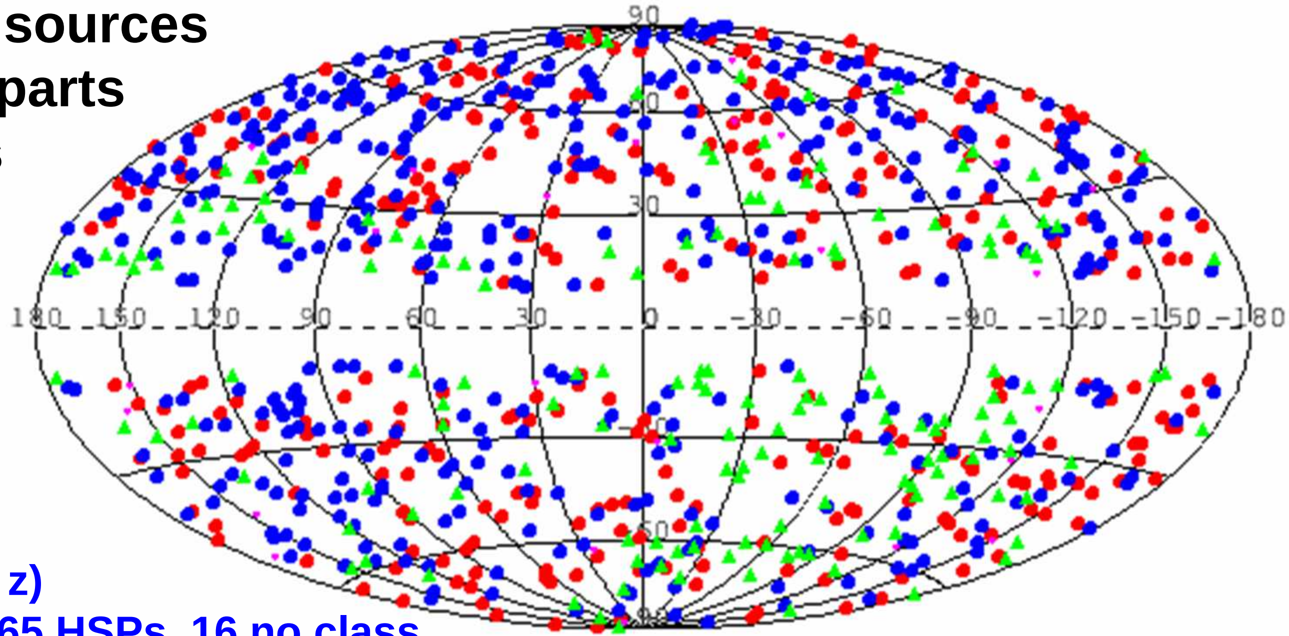

- **Census :**
  - **414 FSRQs**
  - **604 BLLacs**
    (~50% with measured z)
    150 LSPs, 173 ISPs, 265 HSPs, 16 no class.
  - **402 of unknown type (BCUs)**
  - **24 other AGNs**

- **Differences between Northern and Southern Hemispheres:**
  40% of BL Lacs in Southern Hemisphere

Radio galaxies

Non-Blazar and Misaligned AGNs

Name	3FGL	2FGL	1FGL	Type	Photon index
NGC 1218	J0308.6+0408*	...	J0308.3+0403*	FRI	2.07±0.11
IC 310	J0316.6+4119*	J0316.6+4119	...	FRI/BLL	1.90±0.14
NGC 1275	J0319.8+4130*	J0319.8+4130*	J0319.7+4130*	FRI	2.07±0.01
1H 0323+342	J0325.2+3410*	J0324.8+3408*	J0325.0+3403*	NLSy1	2.44±0.12
4C +39.12	J0334.2+3915*	...	...	FRI/BLL?	2.11±0.17
TXS 0348+013	J0351.1+0128*	...	...	SSRQ	2.43±0.18
3C 111	J0418.5+3813	...	J0419.0+3811	FRII	2.79±0.08
Pictor A	J0519.2−4542*	...	...	FRII	2.49±0.18
PKS 0625−35	J0627.0−3529*	J0627.1−3528*	J0627.3−3530*	FRI/BLL	1.87±0.06
4C +52.17	J0733.5+5153	...	...	agn	1.74±0.16
NGC 2484	J0758.7+3747*	...	...	FRI	2.16±0.16
4C +39.23B	J0824.9+3916	...	...	CSS	2.44±0.10
3C 207	J0840.8+1315*	J0840.7+1310	J0840.8+1310	SSRQ	2.47±0.09
SBS 0846+513	J0849.9+5108*	...	...	NLSy1	2.28±0.04
3C 221	J0934.1+3933	...	...	SSRQ	2.28±0.12
PMN J0948+0022	J0948.8+0021*	J0948.8+0020*	J0949.0+0021*	NLSy1	2.32±0.05
PMN J1118-0413	J1118.2-0411*	...	...	agn	2.56±0.08
B2 1126+37	J1129.0+3705	...	...	agn	2.08±0.13
3C 264	J1145.1+1935*	...	...	FRI	1.98±0.20
PKS 1203+04	J1205.4+0412	...	...	SSRQ	2.64±0.16
M 87	J1230.9+1224*	J1230.8+1224*	J1230.8+1223*	FRI	2.04±0.07
3C 275.1	J1244.1+1615	...	...	SSRQ	2.43±0.17
GB 1310+487	J1312.7+4828*	J1312.8+4828*	J1312.4+4827*	agn	2.04±0.03
Cen A Core	J1325.4−4301*	J1325.6−4300	J1325.6−4300	FRI	2.70±0.03
Cen A Lobe	J1324.0−4330e	J1324.0−4330e	J1322.0−4515	FRI	2.53±0.05
3C 286	J1330.5+3023*	...	...	SSRQ/CSS	2.60±0.16
Cen B	J1346.6−6027	J1346.6−6027	...	FRI	2.32±0.01
Circinus	J1413.2−6518	...	...	Seyfert	2.43±0.10
3C 303	J1442.6+5156*	...	...	FRII	1.92±0.18
PKS 1502+036	J1505.1+0326*	J1505.1+0324*	J1505.0+0328*	NLSy1	2.61±0.05
TXS 1613−251	J1617.3−2519	J1617.6−2526c	...	agn	2.59±0.10
PKS 1617−235	J1621.1−2331*	J1620.5−2320c	...	agn	2.50±0.23
NGC 6251	J1630.6+8232*	J1629.4+8236	J1635.4+8228*	FRI	2.22±0.08
3C 380	J1829.6+4844*	J1829.7+4846*	J1829.8+4845*	SSRQ/CSS	2.37±0.04
PKS 2004−447	J2007.8−4429*	J2007.9−4430*	J2007.9−4430*	NLSy1	2.47±0.09

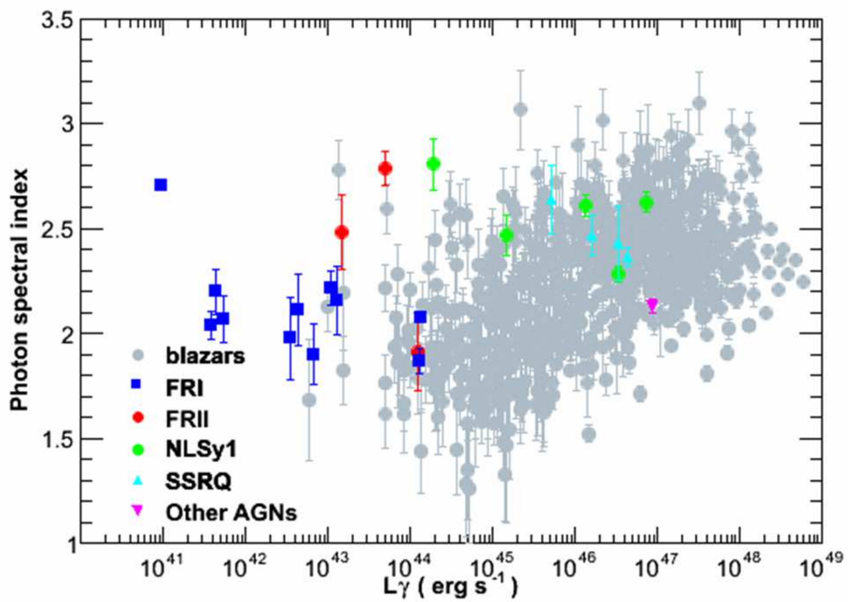

11 FRI
3 FRII | high core dominance
7 SSRQ or CSS
5 Radio-loud NLSyI
6 Other AGNs

CSS: compact steep spectrum
SSRQ: steep-spectrum radio source

Spectral photon index vs photon/energy flux

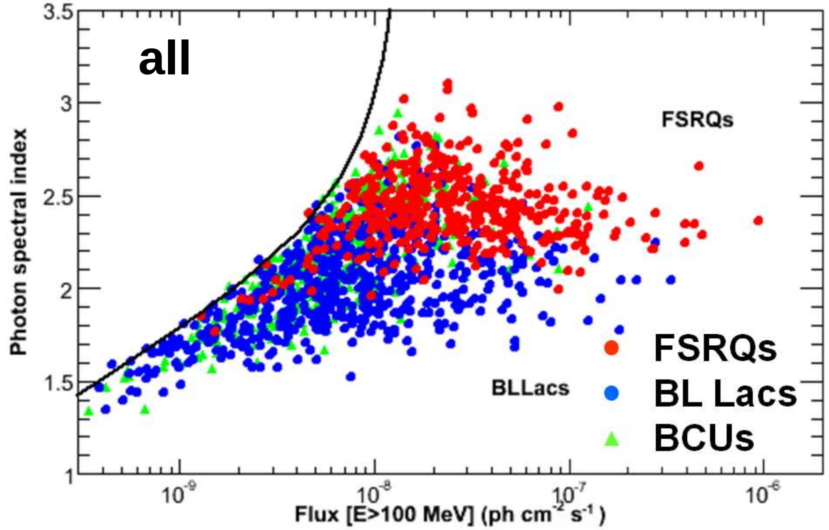

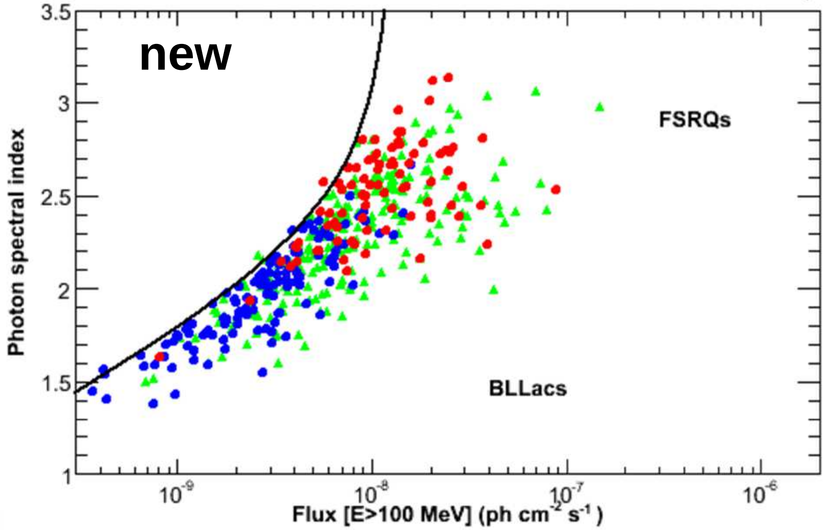

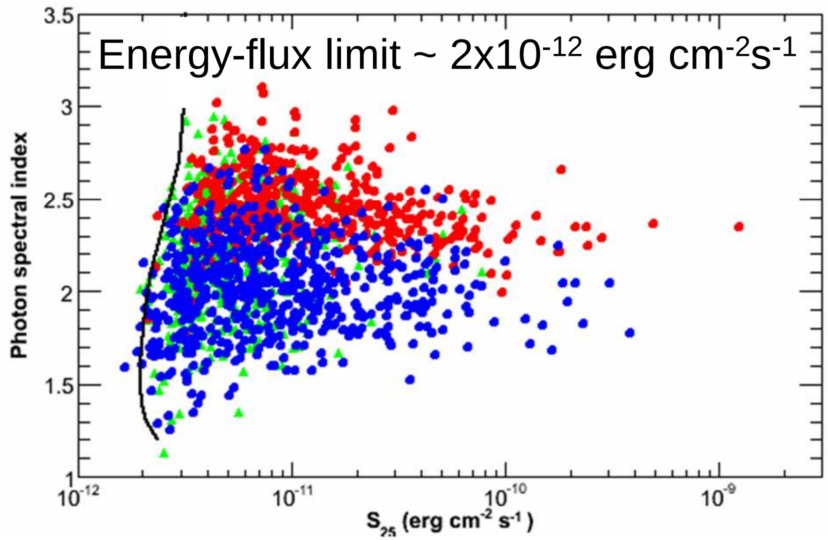

- **Strong bias in photon flux but not in energy flux and thus in luminosity neither**
- **Highest flux in flare: 8x10^{-5} ph cm^{-2}s^{-1} (3C 454.3)**

Redshifts

- slightly higher z for new FSRQs relative to 2LAC ones <z>=1.33 vs. 1.17

- maximum redshift z=3.1

- 295/604 BL Lacs have no measured redshifts (55%, 61%, 40%) for (LSPs, ISPs and HSPs)

- 134 constraints from Shaw et al. (2013)

- Redshift limits for BL Lacs not compatible with measured redshifts: measured redshifts are biased low.

Are many BL Lacs FSRQs with emission lines swamped by the non-thermal continuum?

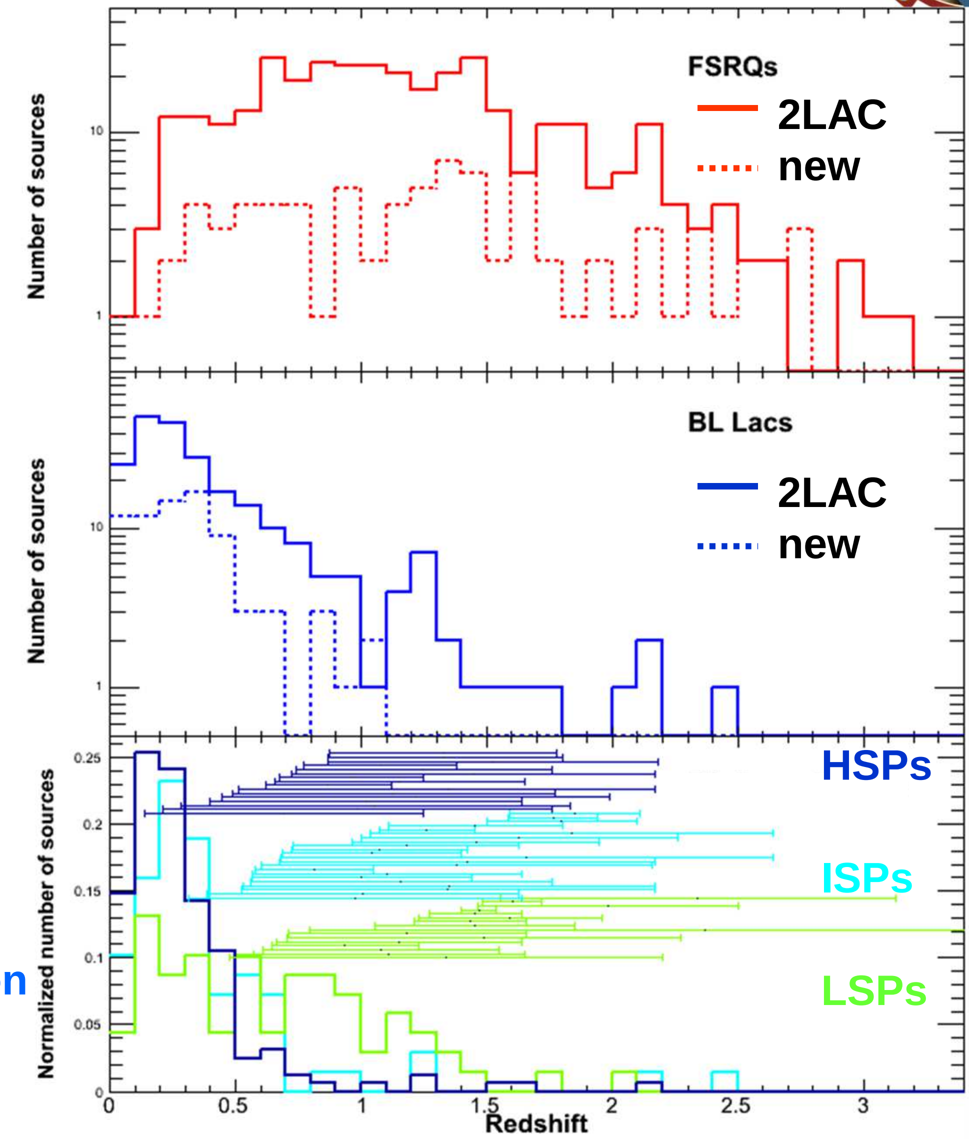

Spectral distributions

Spectral photon index

- Little overlap between FSRQs and BL Lacs
- New FSRQs slightly softer than 2LAC ones: (<Γ>=2.53 vs. 2.41), not so for BL Lacs
- Lowest index~1.5, as predicted by shock-acceleraton models
- BCUs index distribution straddling the two classes' and extending beyond 2.5

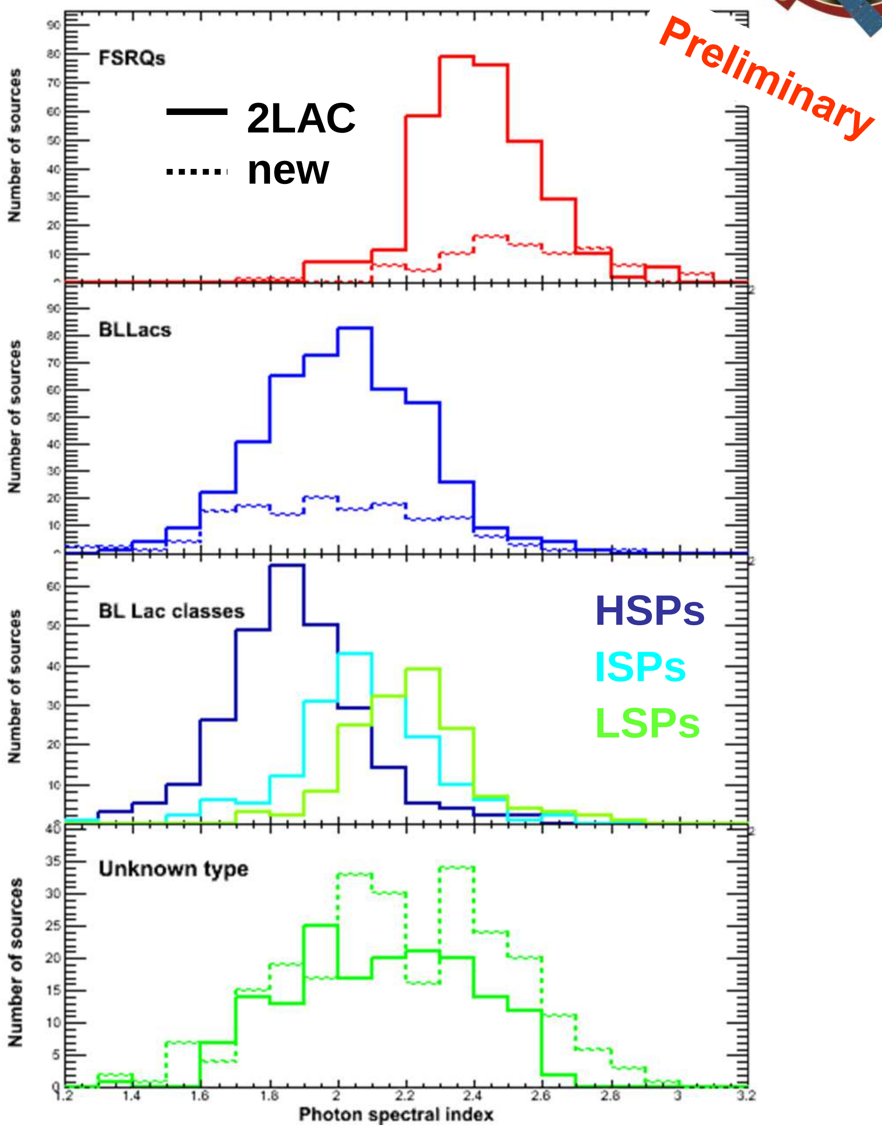

ν_{peak} vs. photon index

Correlation between photon spectral index measured with the LAT and position of the SED synchrotron peak

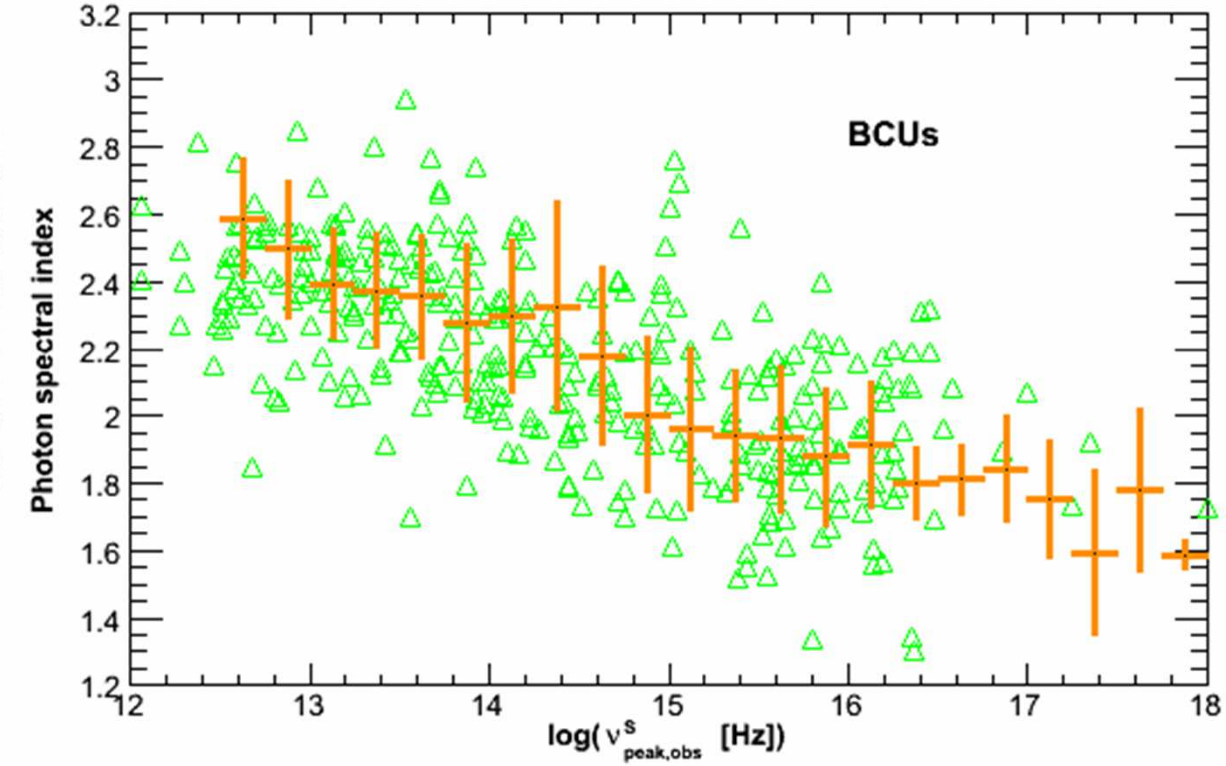

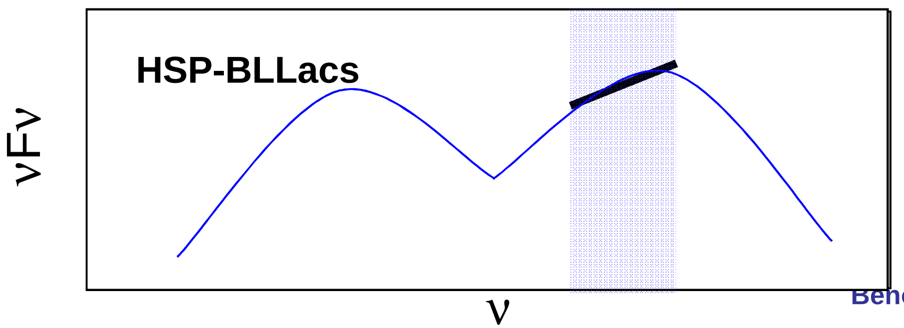

Spectral curvature

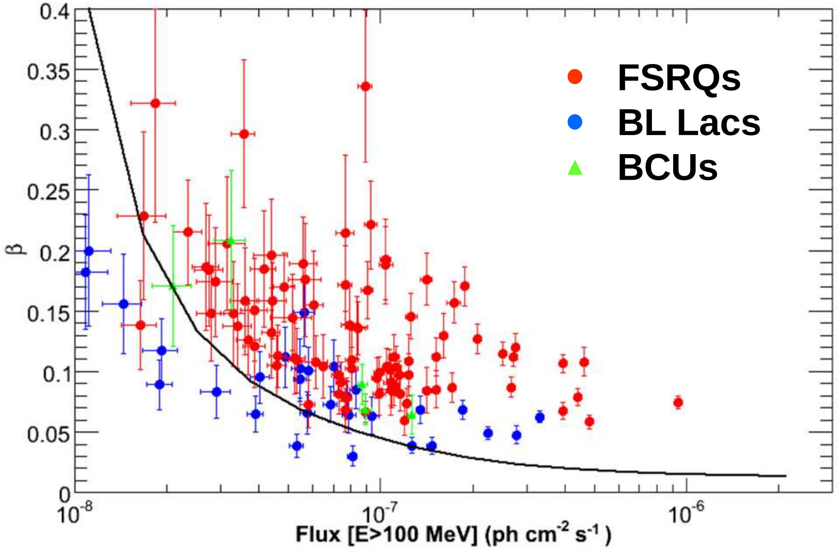

$$N(E) = N_0 \left(\frac{E}{E_0}\right)^{-\alpha-\beta \log(\frac{E}{E_0})}$$

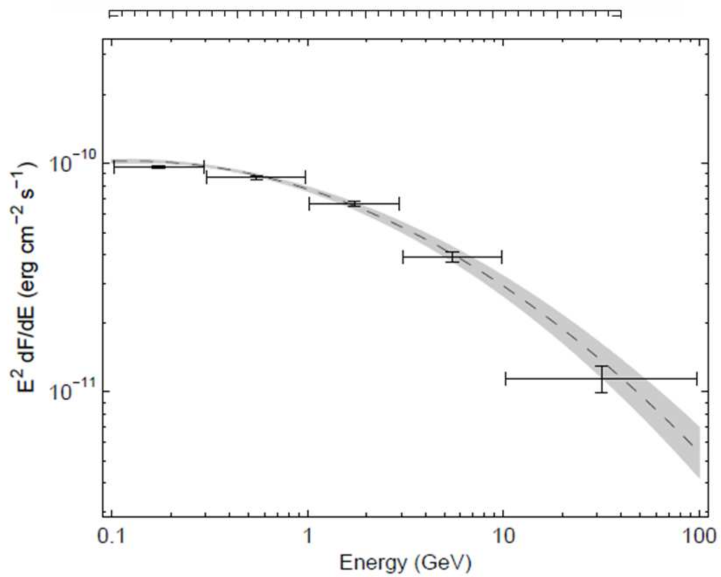

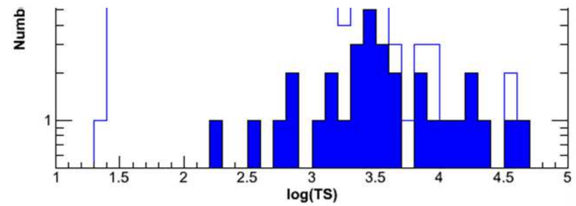

Feature first seen in 3C 454.3
91 FSRQs, 32 BL Lacs, 8 BCUs show significant spectral curvature

Abdo +09, Poutanen & Stern 10, 14, Cerruti+13, Dermer+14, Finke & Dermer 13, Hunger & Reimer 15 Kohler & Nalewajko 15

- **γγ-absorption**
- **superposition of different EC components**
- **superposition of different flares**
- **intrinsic curvature of electron energy distribution**

Luminosities

Redshift versus luminosity

$$L_\gamma = 4\pi d_L^2 \frac{S(E_1,E_2)}{(1+z)^{2-\Gamma}}$$

d_L: luminosity distance
$S(E_1,E_2)$: energy flux between E_1(100 MeV) and E_2 (100 GeV)

Only bright sources are visible at large distance
Malmquist bias

Distant HSPs at constant luminosity couldn't be detected

Cautionary note:
only half of the BLLacs have measured redshifts

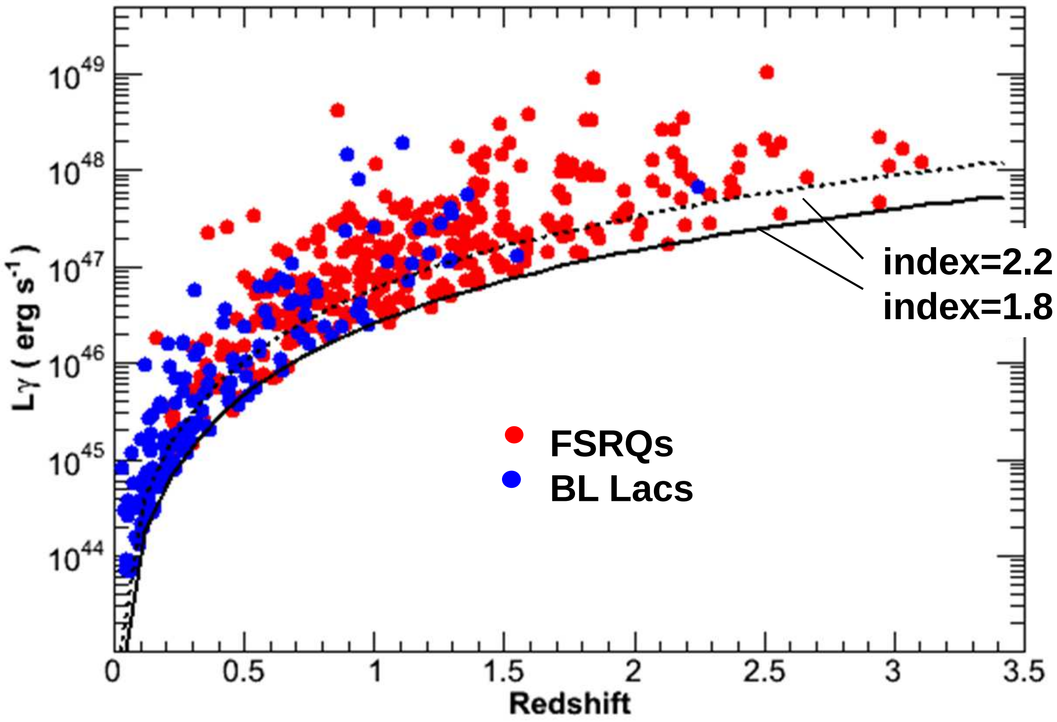

Blazar Sequence: « Grand Unification » between BL Lacs and FSRQs?

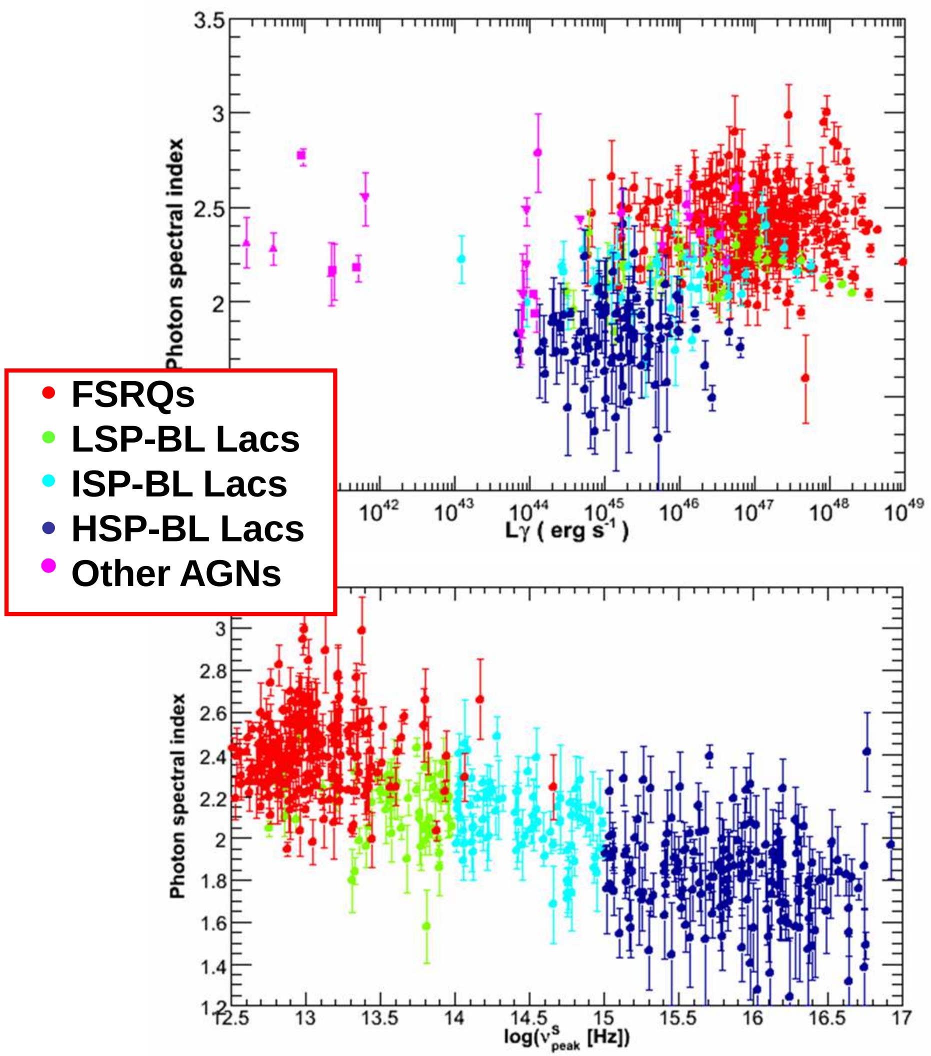

Correlation between luminosity and photon index, Compton dominance: Blazar sequence?

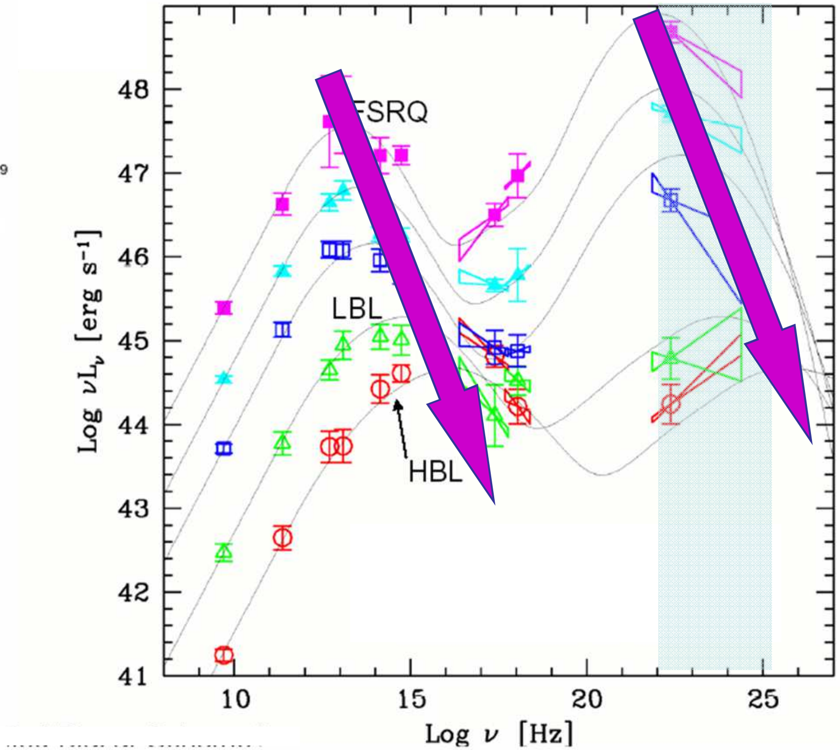

Donato+ (2002) Fossati+(1998)

Luminosity vs photon index

Change of accretion regime at 10^{46} erg s^{-1}? (Ghisellini et al. 09)
⇒different disk solutions
- **α-disks** (Shakura-Sunyaev) **in FSRQs**
- **ADAFs in BLLacs**

⇒electron cool more efficiently in stronger ambiant radiation fields
IC hump peaks at lower energy

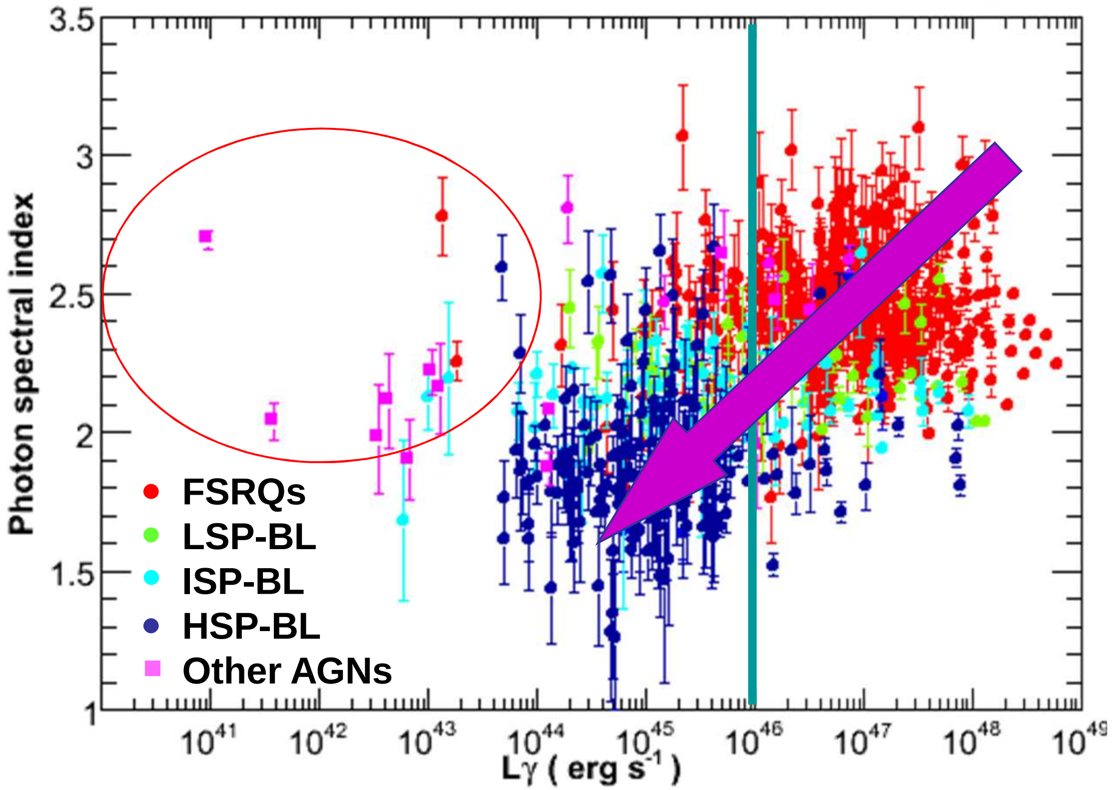

Reduced accretion rate leading to an evolutionary link between classes:
FSRQ →LSP BLLacs →HSP BLLacs
as the fuel gets progressively exhausted
(Ghisellini et al., Boettcher and Dermer, Cavaliere and D'Elia)

Variability

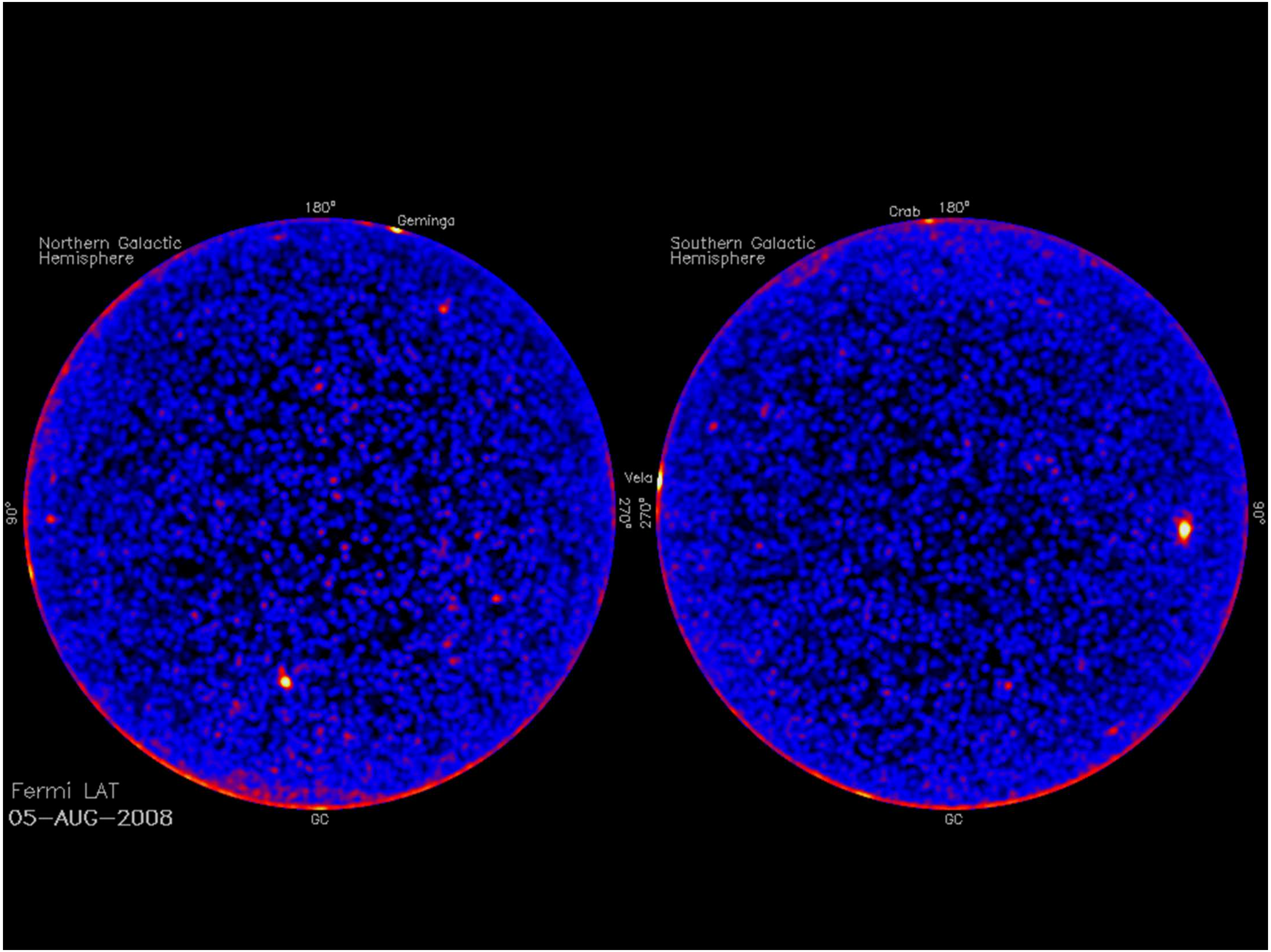
180°
Geminga
Northern Galactic
Hemisphere
90°
270°
Vela
Fermi LAT
05-AUG-2008
GC
Crab
180°
Southern Galactic
Hemisphere
270°
90°
GC

Fermi's variable sky

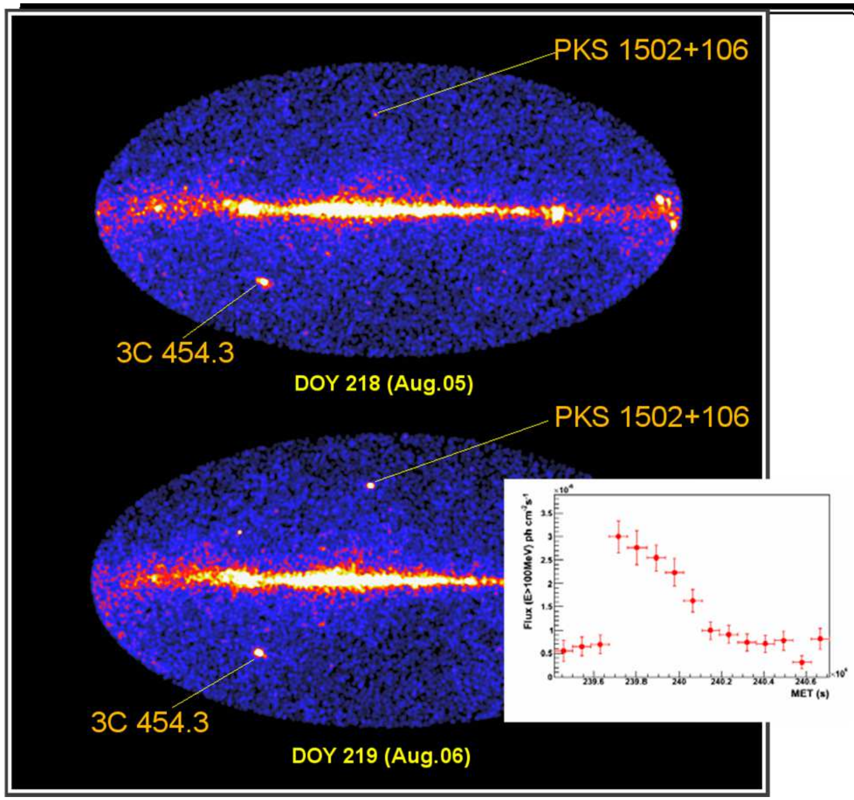

~370 Astronomers telegrams

~65% about AGNs

alert threshold:

F[E>100 MeV]~10^{-6} ph cm^{-2} s^{-1}

Other considerations:

- **Significant flux rise wrt average**
- **TeV detectability**
- **Event rarity**

http://www-glast.stanford.edu/cgi-bin/pub_rapid

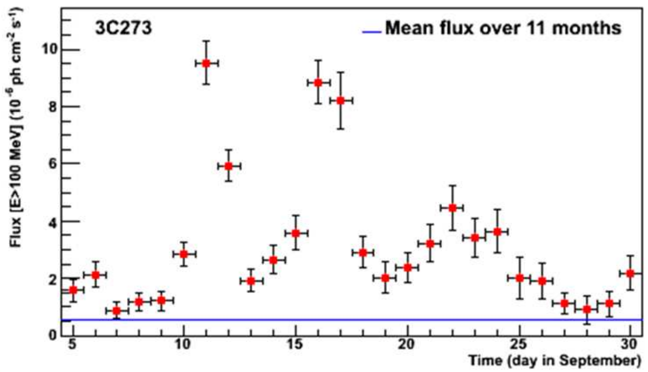

Flare Advocates issue alerts and feed the Fermi blog

Variability

- **Variability index distributed as a χ^2 with 47 d.o.f. for non-variable sources.**
- **Fractions of sources showing significant variability**
  FSRQs: 69%   BL Lacs: 23%
  (39%, 23%, 15%) for (LSP, ISP,HSP)
- **The LAT samples different parts of the high-energy hump for the different classes.**
- **Monthly light curves to be extended beyond 48 months, continuously updated and posted on the ASDC site**

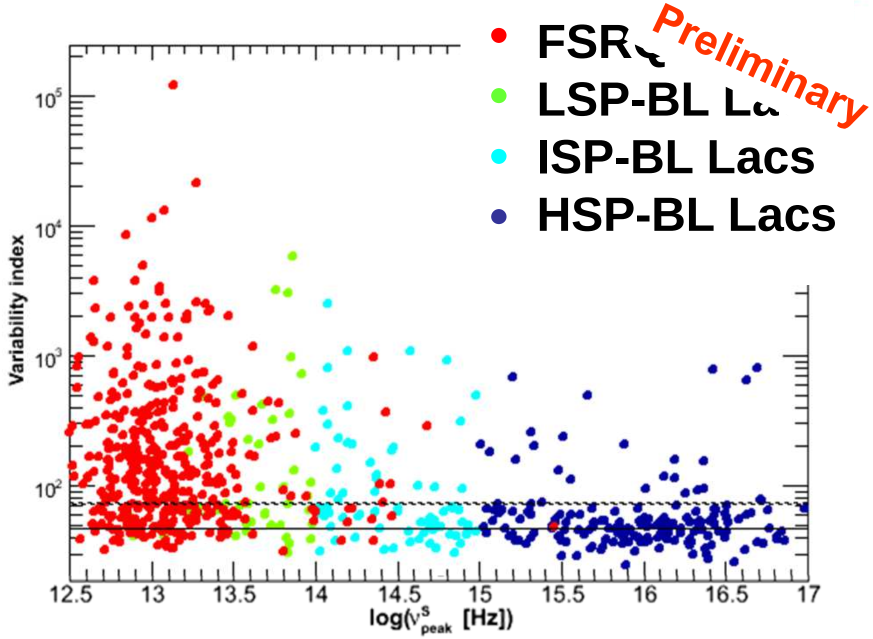

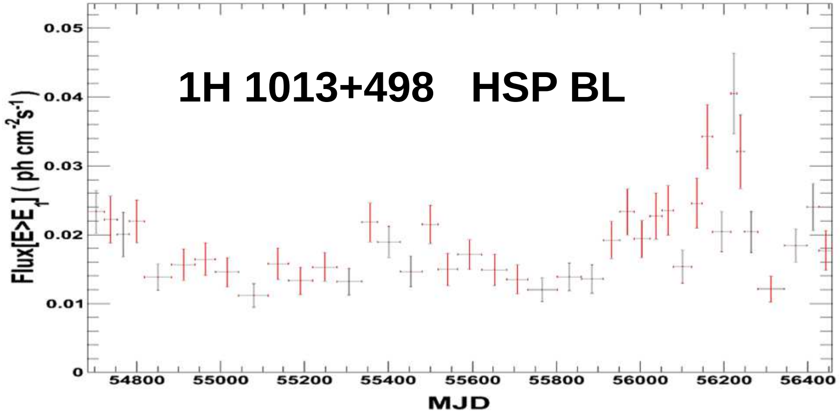

Shortest timescales

Constraints on size and location of emitting zone . $R < 2\Gamma^2 c\Delta t_{\rm var}$

5 sources show T_{min} lower than 3 hr:
3C 454.3, 3C 273, 4C+21.35, PKS 1510-089, 3C 279
$R_S/c \sim 10^4\ M_9$ s

Sub-hour variability (<20 min) is found for 3C 454.3, PKS 1510-089 and 3C 279
Indication that emission takes place

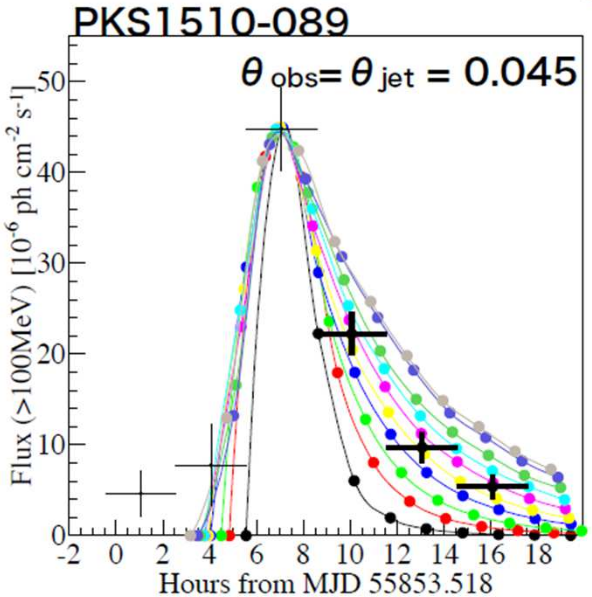

Saito+ 13

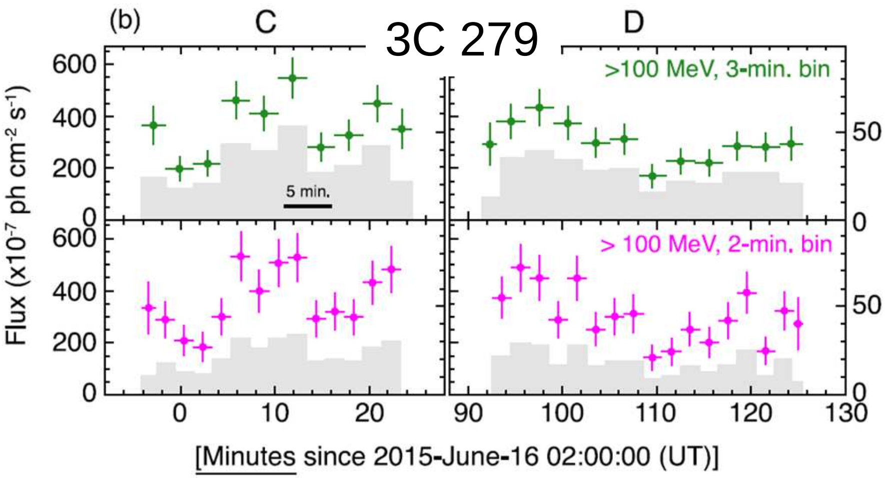

Ackermann+ 16

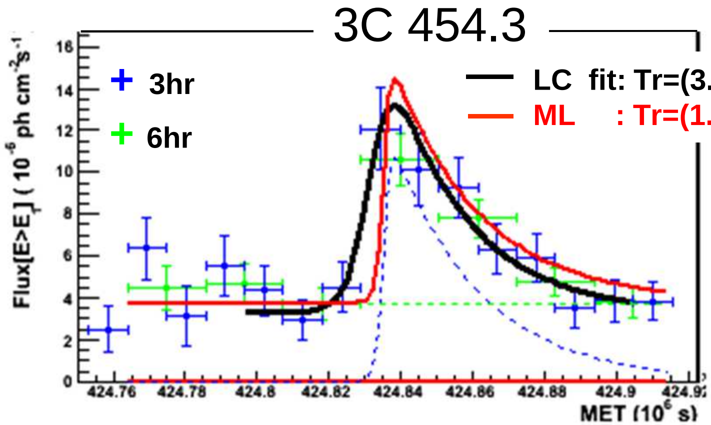

Britto+ 16

PG 1553+113

HSP BL Lac
0.395 < z < 0.62
one of the brightest BL Lacs in the X-ray band
TeV source (HESS, MAGIC)

Indication for a periodic behavior in

- **the radio (15 GHz)**
- **the optical (R-band)**
- **the LAT band**

Autocorrelation gives a peak at 750 days

Interpretation:

- **binary black hole?**
- **warped disk?**
- **other?**

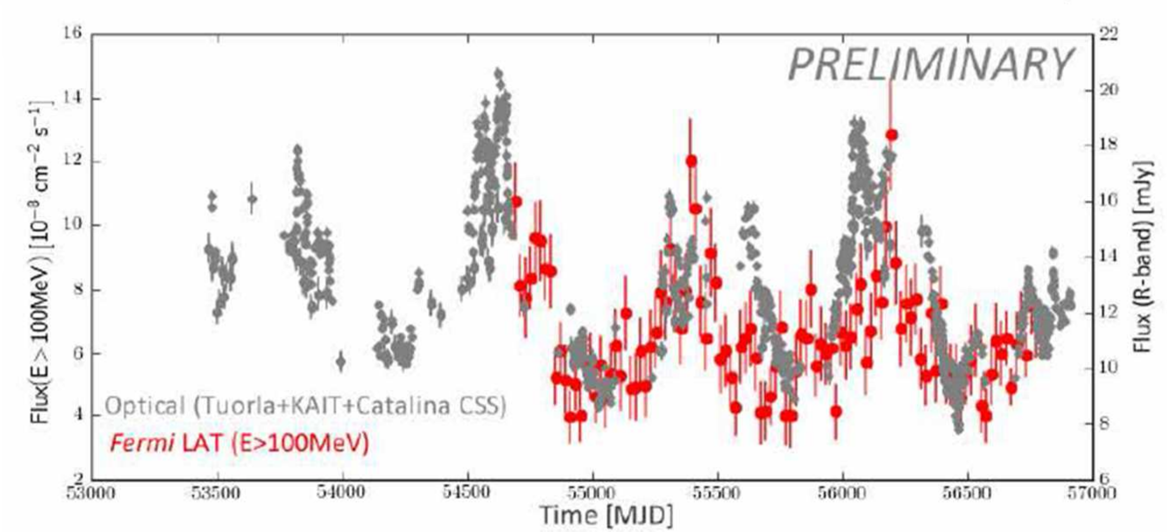

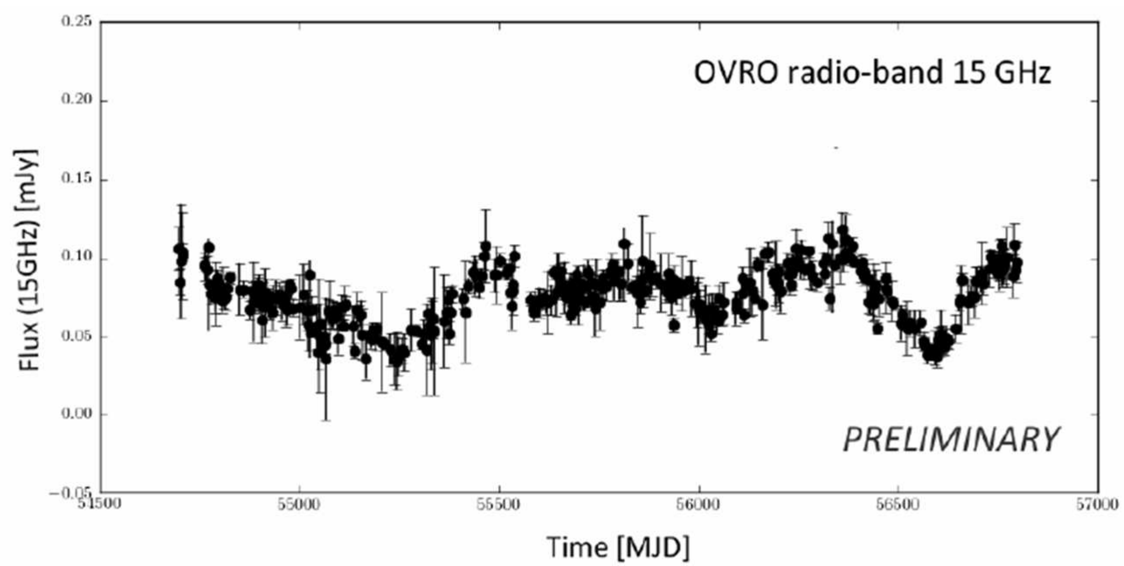

Power density spectrum

$$|F_N(\nu)|^2 = \left(\sum_{i=1}^{N} f(t_i)\cos(2\pi\nu t) \right)^2 + \left(\sum_{i=1}^{N} f(t_i)\sin(2\pi\nu t) \right)^2$$

PDS ~ 1/freq$^{-\alpha}$ with α between 1 (« flicker », « pink-noise ») and 2 (« shot noise », «Brownian») with peak around 1.6-1.7 (similar to optical or radio)

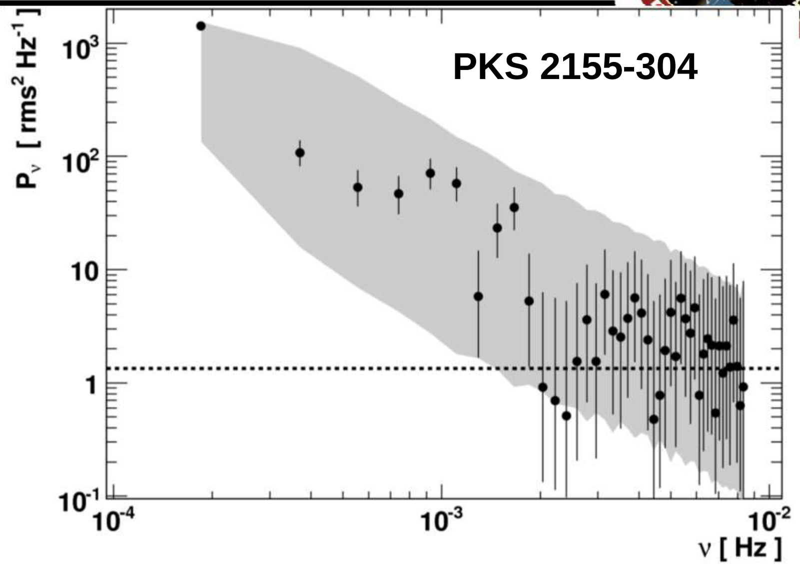

Aharonian et al 07

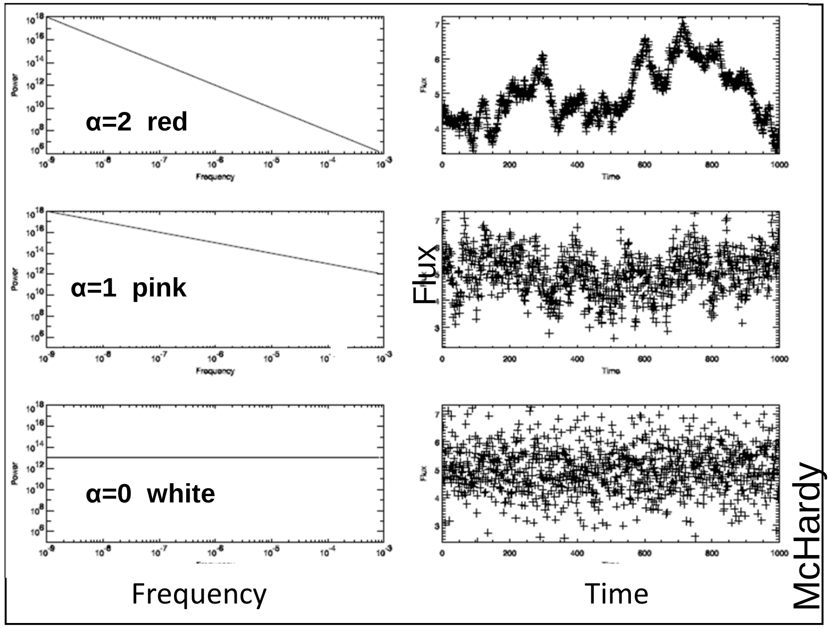

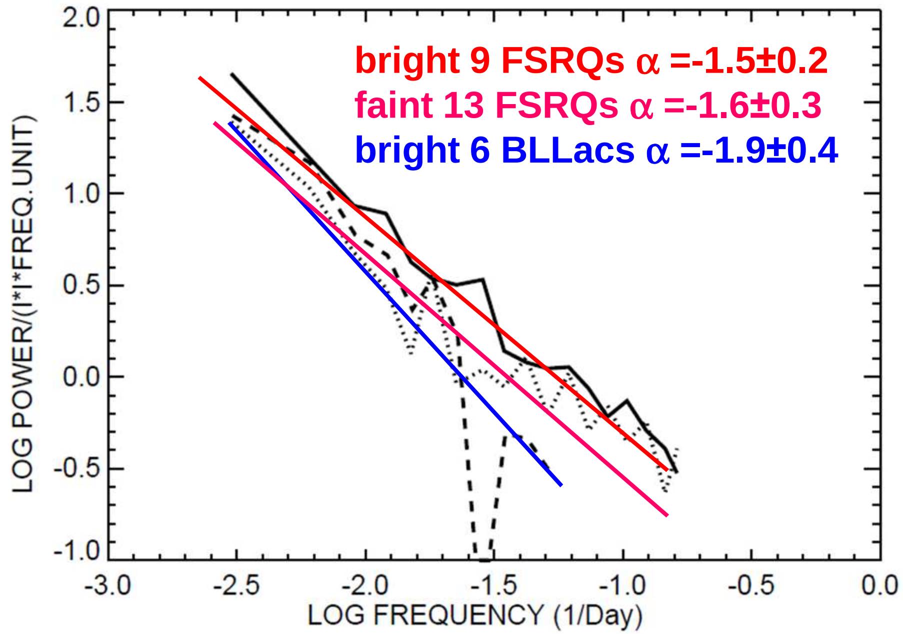

Abdo et al 10

Log N-Log S
Contribution to
Extragalactic Diffuse Background

log N-log S

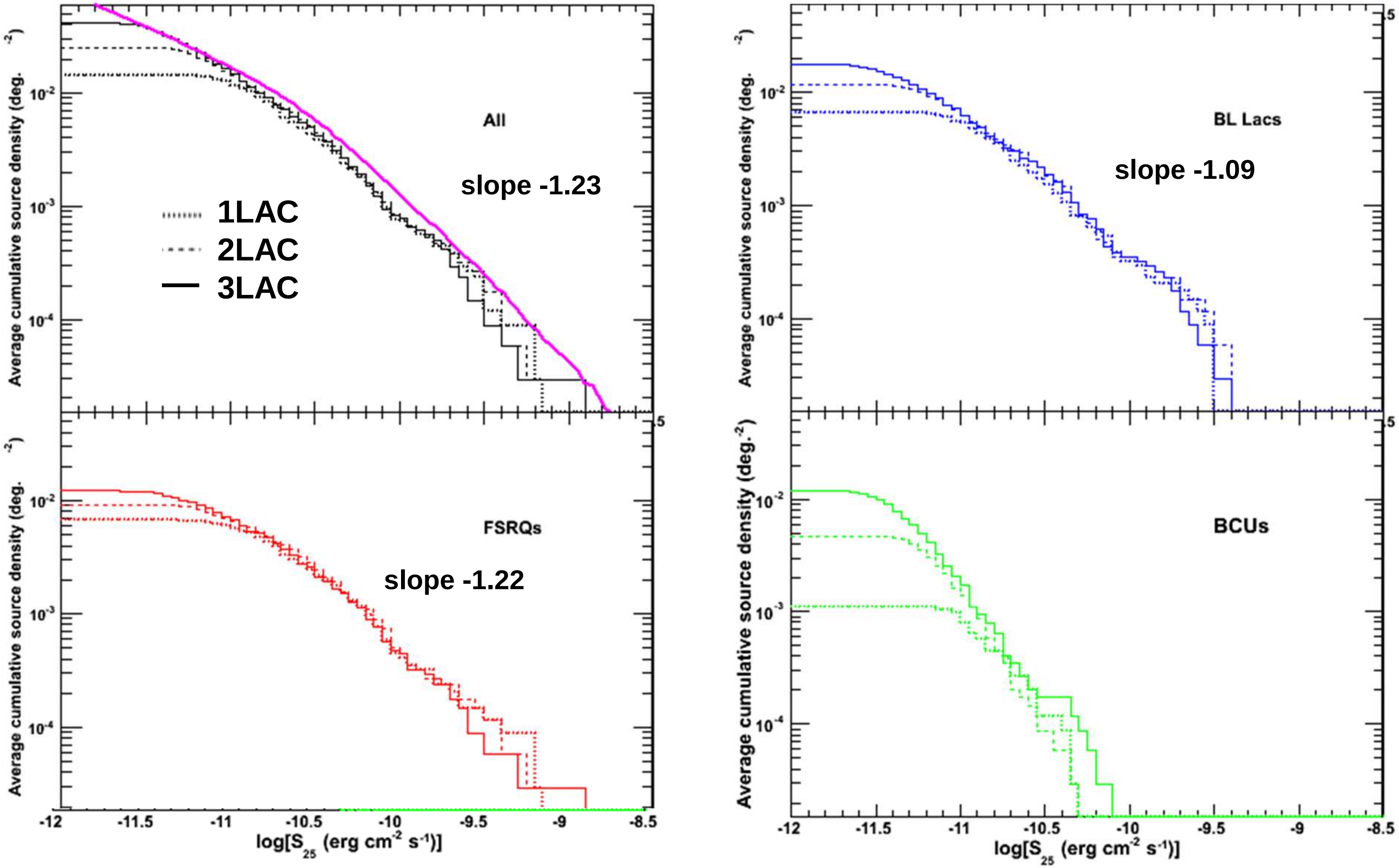

Allows the contribution of blazars to the diffuse gamma-ray background to be estimated

Contribution to Extragalactic Gamma-Ray Background

EGB total intensity of 1.1×10^{-5} ph cm^{-2} s^{-1} sr^{-1}

Blazars contribute a grand-total of (5-7)× 10^{-6} ph cm^{-2} s^{-1} sr^{-1}

– Resolved sources : ~4× 10^{-6} ph cm^{-2} s^{-1} sr^{-1}

– Unresolved blazars: ~(2-3)×10^{-6} ph cm^{-2} s^{-1} sr^{-1} (in agreement with Abdo+10)

Blazars, star-forming galaxies and radio galaxies can explain the intensity and the spectrum of the EGB

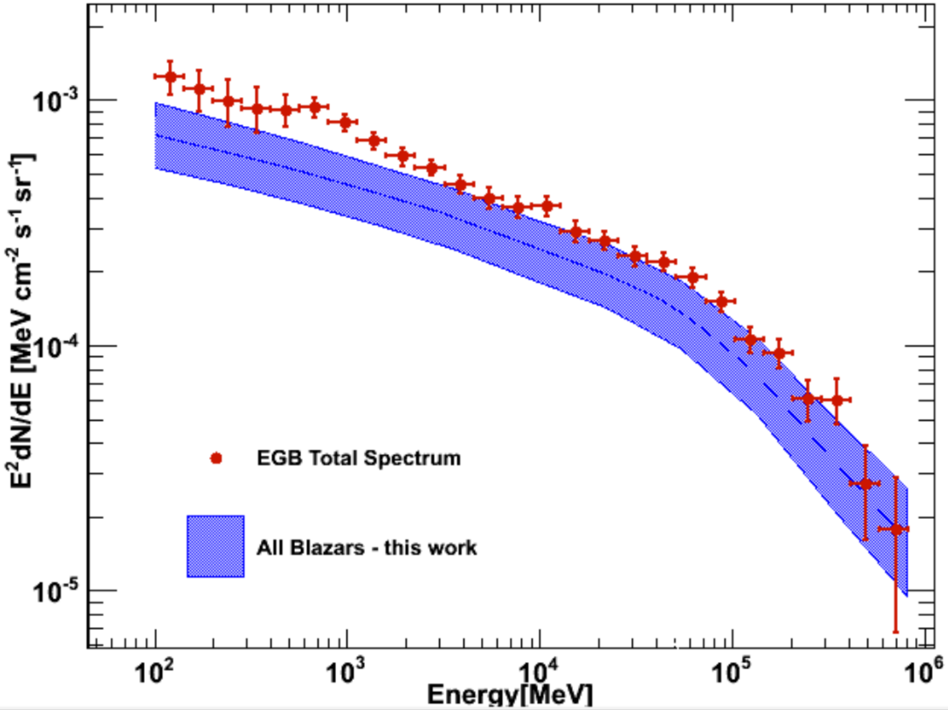

Ajello+ 14

Blazar luminosity functions

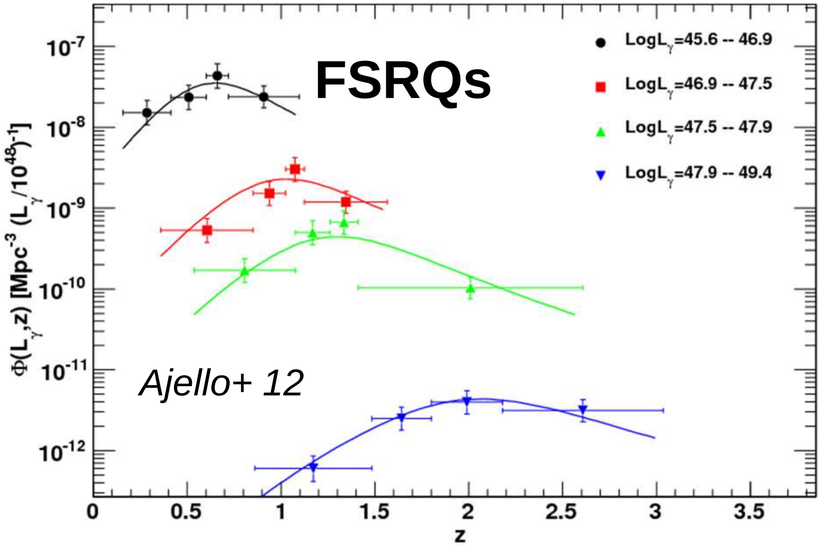

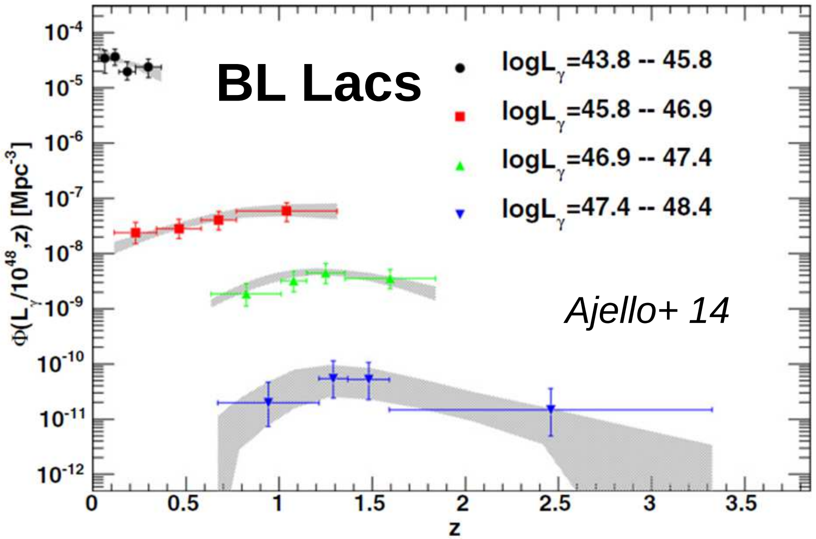

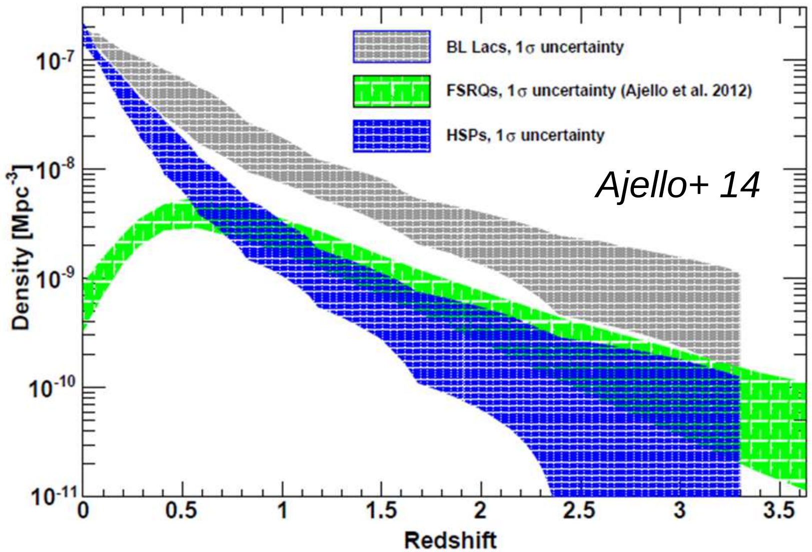

- **Rise in HSP-BL Lac density corresponds to a drop-off in FSRQ density**
- **Evolution of FSRQS into HSPs due to starvation of accreting mattter?**

Correlations with other wavelenghts

Connection with BZCat

LAT-detected fraction: 24% (409/1707) for FSRQs, 44% (543/1221) for BL Lacs and 27% (59/221) for AGUs

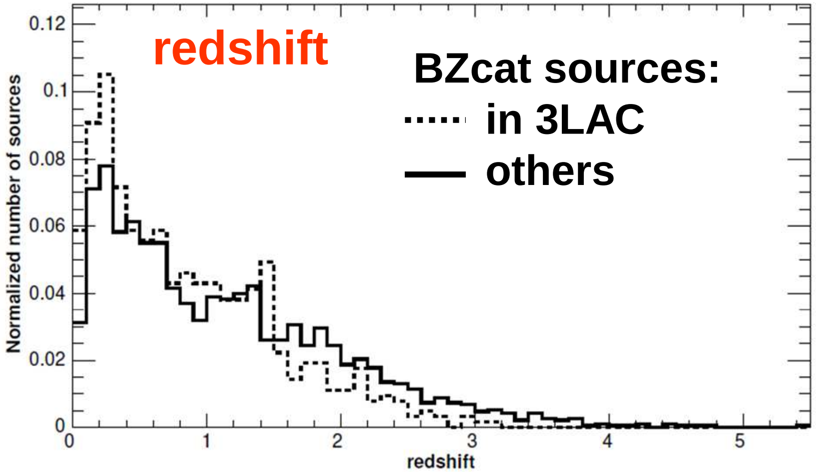

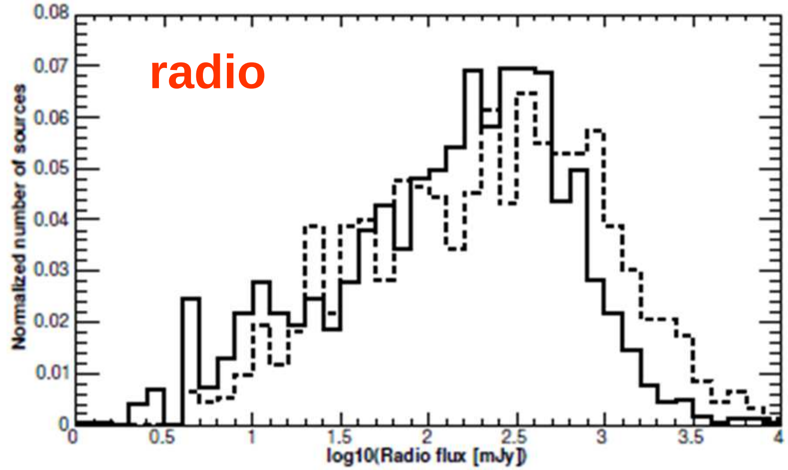

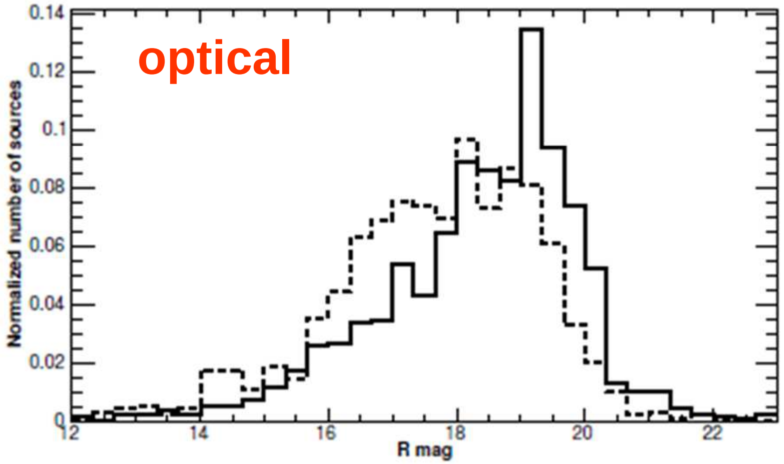

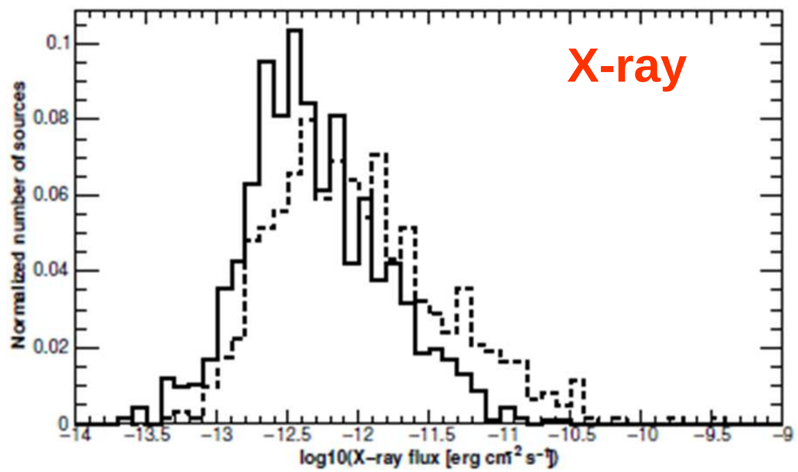

Synergy with neighboring bands

Preliminary

- **85 3LAC sources in the Swift BAT 70-month survey**
  only 9 BAT FSRQs and 7 BL Lacs missing in 3LAC

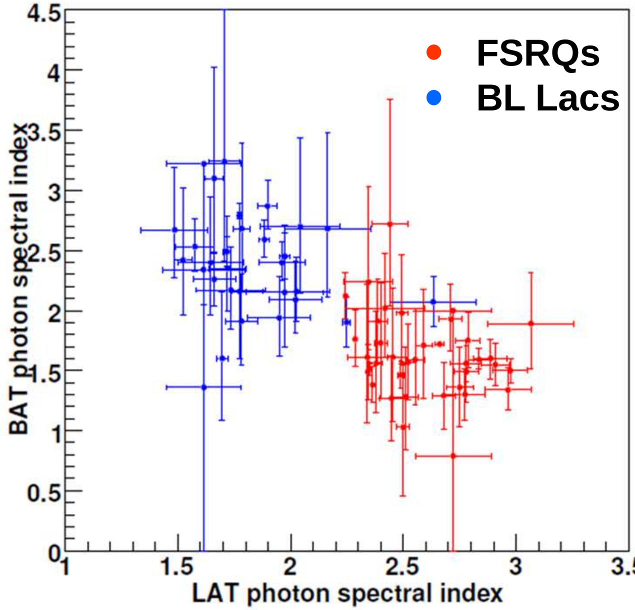

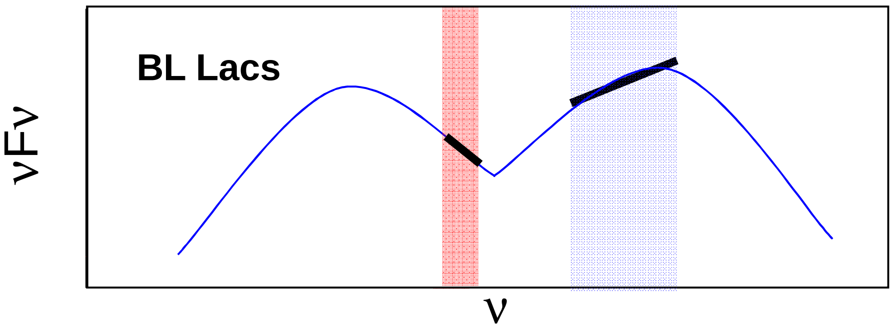

- **55 out of 56 TeV AGNs in 3LAC**
  28 found to be variable

- **96 3LAC AGNs in the V38 INTEGRAL Cat.**

Table 10. Properties of the VHE AGN detected by the *Fermi* LAT.

VHE Name	3FGL Name	Source Class	SED Type	Redshift	Spectrum Type[a]	1FGL/1FHL[b]
SHBL J001355.9−185406	J0013.9−1853	BL Lac	HSP	0.095	PL	···
KUV 00311-1938	J0033.6-1921	BL Lac	HSP	>0.51	PL	H
RGB J0136+391	J0136.5+3905	BL Lac	HSP	···	PL	H
RGB J0152+017	J0152.6+0148	BL Lac	HSP	0.08	PL	Y
3C 66A	J0222.6+4301	BL Lac	ISP	$0.3347 < z < 0.41$	LP	Y
1ES 0229+200	J0232.8+2016	BL Lac	HSP	0.139	PL	···
PKS 0301-243	J0303.4-2407	BL Lac	HSP	0.26	PL	H
IC 310	J0316.6+4119	Radio Gal	HSP	0.018849	PL	Y
RBS 0413*	J0319.8+1847	BL Lac	HSP	0.19	PL	Y
NGC 1275*	J0319.8+4130	Radio Gal	ISP	0.018	LP	Y
1ES0347−121	J0349.2−1158	BL Lac	HSP	0.188 (?)	PL	···
1ES 0414+009	J0416.8+0104	BL Lac	HSP	0.287	PL	Y
PKS 0447−439	J0449.4−4350	BL Lac	HSP	0.205	PL	Y
1ES 0502+675*	J0508.0+6736	BL Lac	HSP	0.341	PL	Y
PKS 0548-322	J0550.6−3217	BL Lac	HSP	0.069	PL	H
1ES 0647+250	J0650.7+2503	BL Lac	HSP	···	PL	H
RGB J0710+591 (1H 0658+595?)	J0710.3+5908	BL Lac	HSP	0.125	PL	Y
S5 0716+714	J0721.9+7120	BL Lac	ISP	$0.2314 < z < 0.27$	LP	Y
1ES 0806+524	J0809.8+5218	BL Lac	HSP	0.138	PL	Y
RX J0847.1+1133 (RBS 0723)	J0847.1+1134	BL Lac	HSP	0.199	PL	···
1RXS J101015.9-311909	J1010.2-3120	BL Lac	HSP	0.143	PL	H
1ES 1011+496	J1015.0+4925	BL Lac	HSP	0.212	PL	Y
1ES 1101−232	J1103.5−2329	BL Lac	HSP	0.186	PL	Y
Markarian 421	J1104.4+3812	BL Lac	HSP	0.031	PL	Y
Markarian 180	J1136.6+7009	BL Lac	HSP	0.046	PL	Y
1ES 1215+303	J1217.8+3007	BL Lac	HSP	···	PL	Y
1ES 1218+304	J1221.3+3010	BL Lac	HSP	0.182	PL	Y

radio/γ–ray connections with VLBA

The jets of the LAT-detected blazars have:

- higher-than-average apparent speeds (Lister+09, Piner+12),
- larger-than-average apparent opening angles (Pushkarev+09)
- more compact radio cores (Kovalev+09)
- strong polarization near the base of the jet (Linford+11)
- higher variability Doppler factors (Savolainen+10).

All the above points to higher-than-average Doppler boosting in γ-ray bright blazars.

AGN jets have been found to be in a more active radio state within several months of the LAT-detection of their strong γ-ray emission (Kovalev+09, Pushkarev+10). The γ-ray photon flux correlates with the parsec-scale radio flux density (Kovalev+09; Arshakian +11)

γ-ray loudness correlates with position of synchrotron peak and gamma-ray photon spectral index for BL Lacs (Lister+12, Linford+12)

Radio-gamma-ray connection

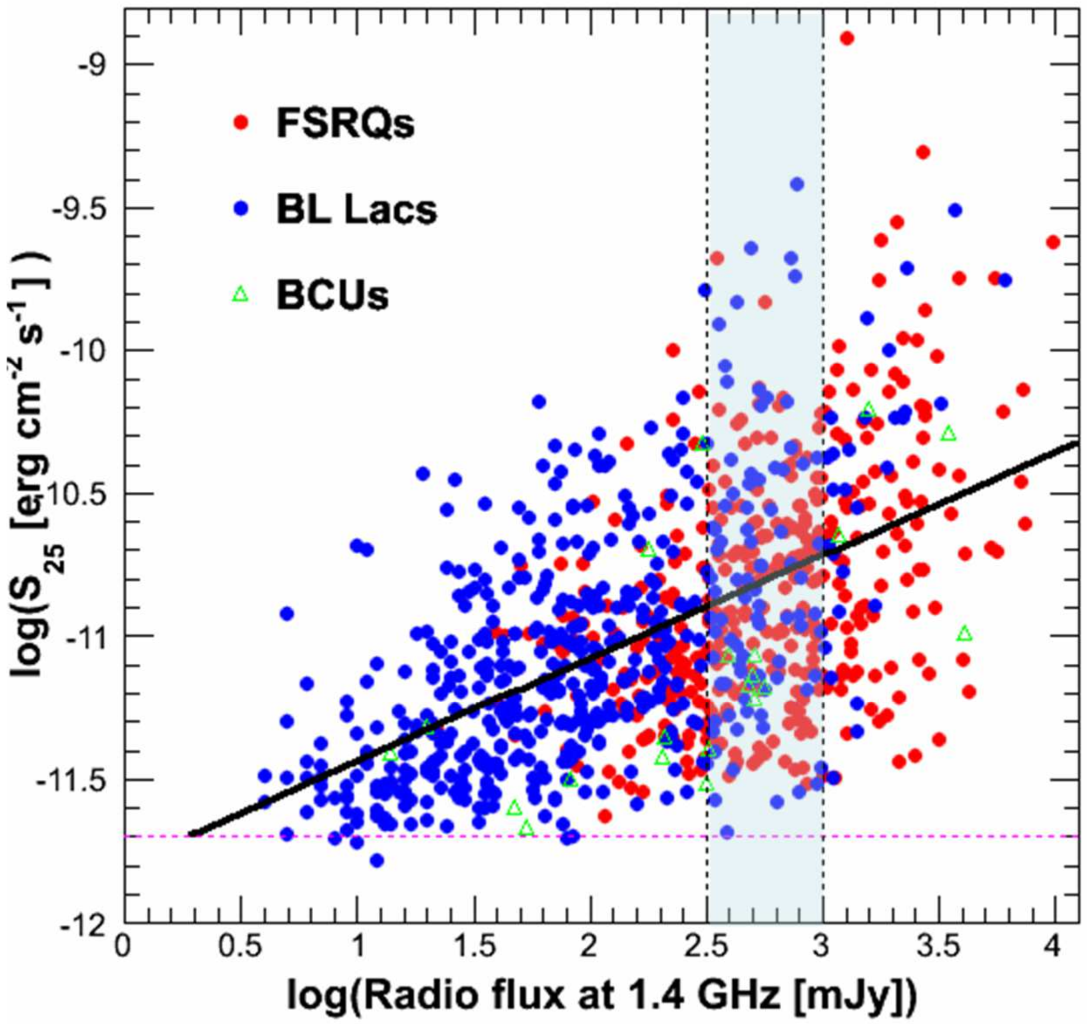

Pearson coefficient: 0.52

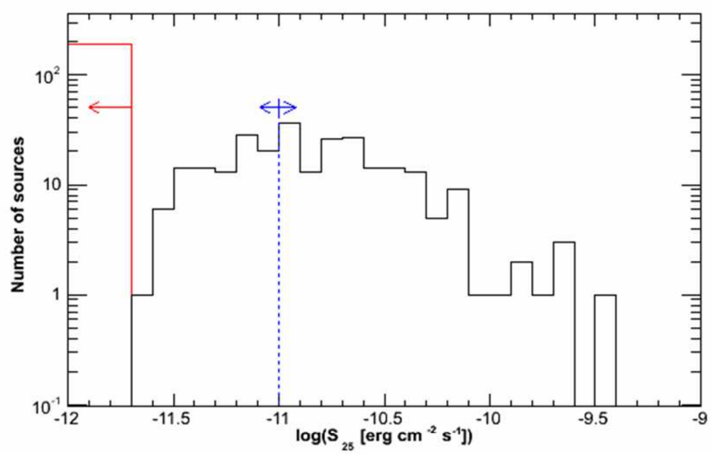

Location of emission zone: close or far from BH?

« Near » scenario

- **Fast variability**
- **Seed photons (disk, BLR, torus) for External Compton**

«Distant » scenario (outside of BLR to pc scales):

- **majority of γ-flares associated with new superluminal knots (but travel time effects)**
- **coincidences between radio and gamma-ray flares**
- **detection of > 100 GeV photons in some FSRQs**
- **no absorption features in SED from BLR photons**

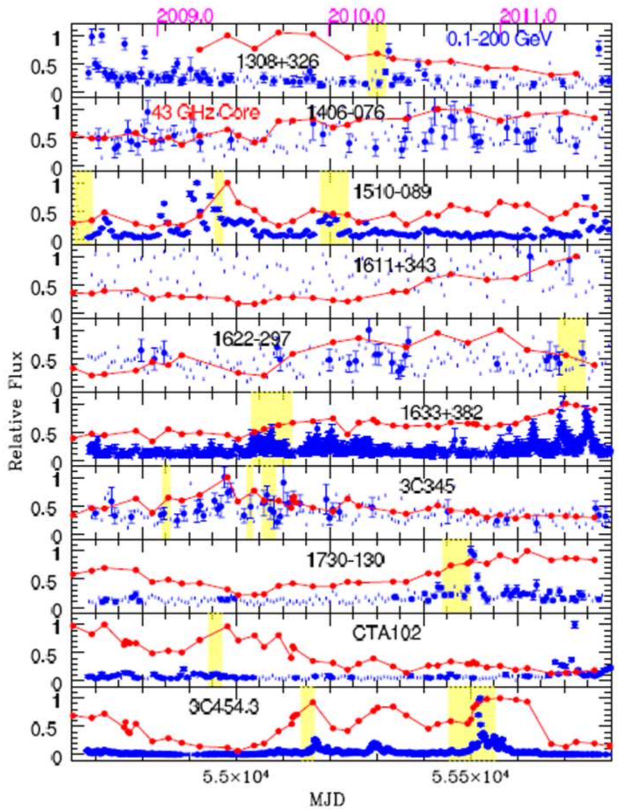

A. Marscher+ 11

34 γ-bright blazars and radio-galaxies

Fermi LAT γ–ray, 43 GHz VLBI "core

times of new superluminal knot passing the core

Strong challenges to theoretical models!

Extragalactic Background Light

Extragalactic Background Light

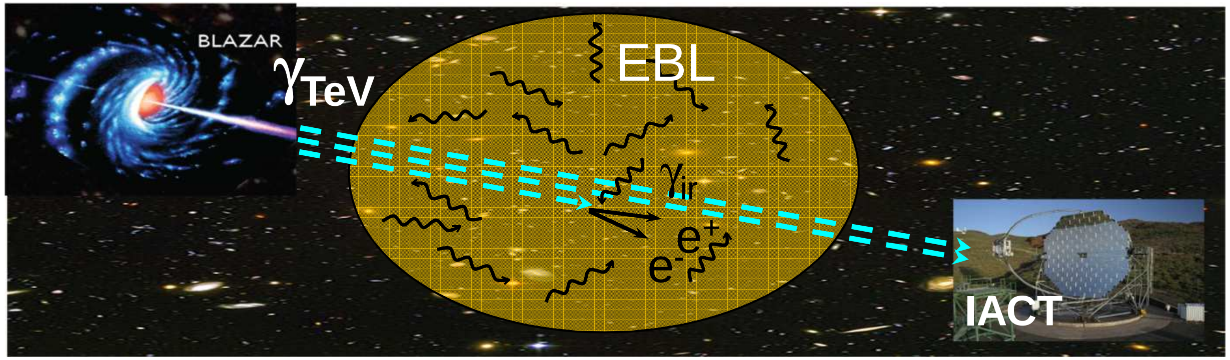

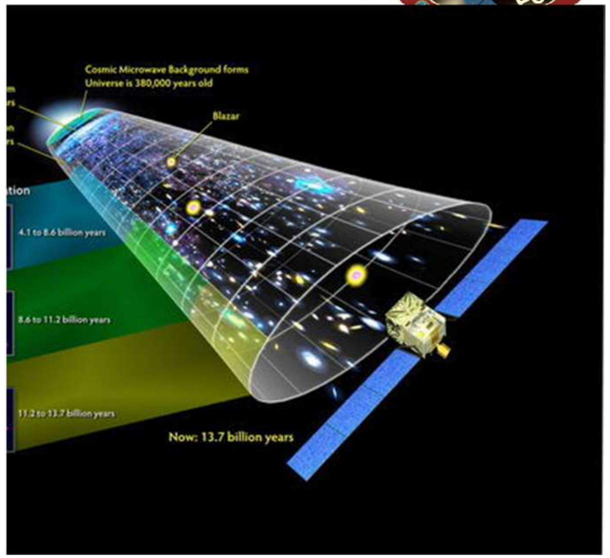

total stellar radiation emitted by galaxies through the Universe history

- redshifted by the Universe expansion
- reprocessed (absorption-reemission) by dust

Direct measure difficult (zodiacal light)

$$\gamma + \nu_{IR} \rightarrow e^+ e^-$$

$$\text{threshold}: \quad \varepsilon E\,(1+z)^2(1-\cos\theta) > 2(m_e c^2)^2$$

$$\varepsilon_{eV} = \frac{500\text{GeV}}{E_{GeV}(1+z)^2} \quad \text{or} \quad \lambda_{\mu m} = 1.2\frac{E_{GeV}(1+z)^2}{500\text{GeV}}$$

$$F_\nu^{obs} = F_\nu^0 \exp(-\tau(\nu, z))$$

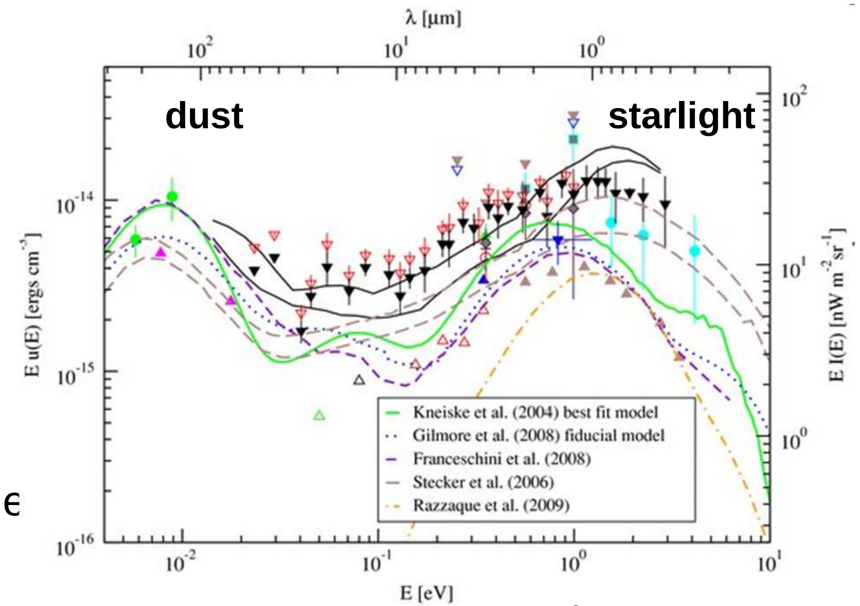

Measurement of EBL density
EBL density compatible with lower limits obtained by the integrated light of resolved galaxies.

EBL studies

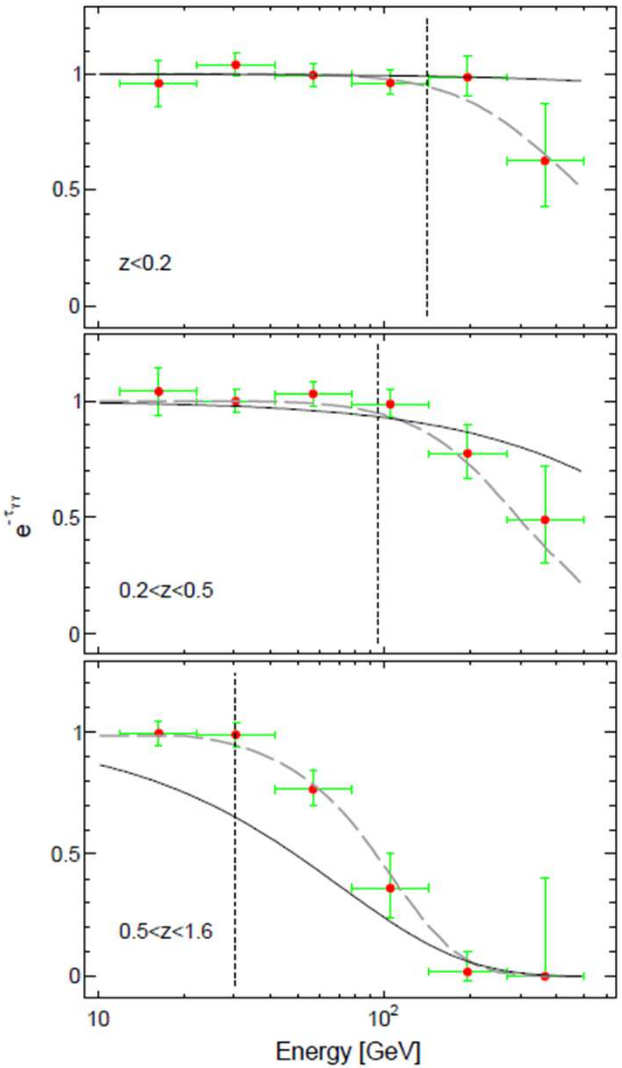

Ackermann et al. 2012Sci...338.1190A

Attenuation effect in 150 2LAC BL Lac spectra
Compatible with low-opacity models
UV photons E> 5 eV

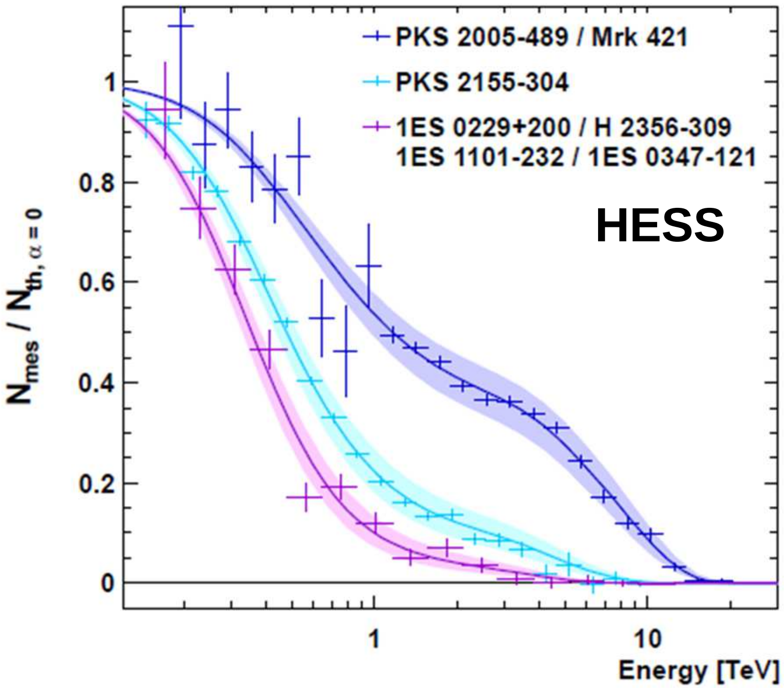

Second Fermi Hard-Source List (2FHL)

360 sources at E>50 GeV

- Spectral indices softer than in 3FGL, 1FHL on average

- Softening with increasing redshift , indicative of EBL attenuation

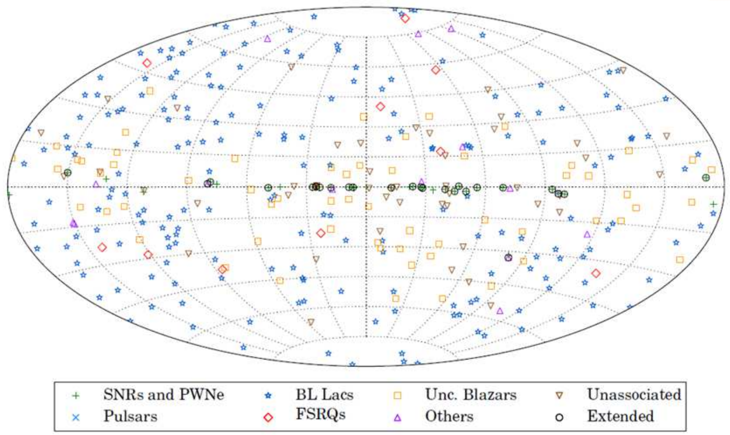

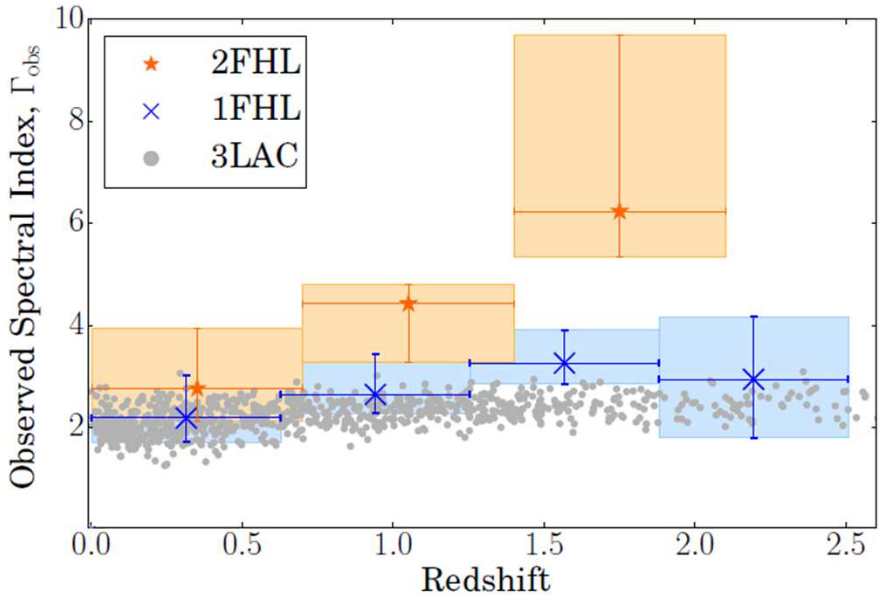

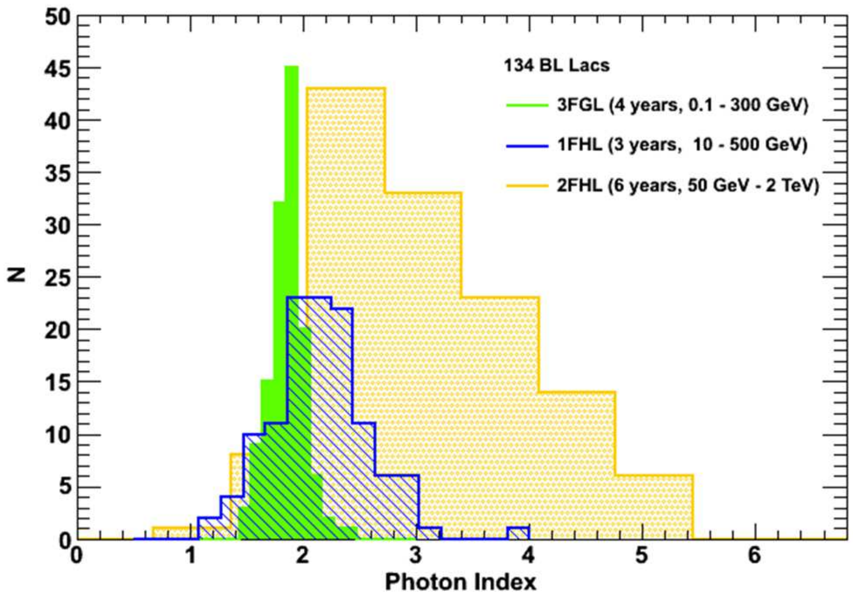

Summary

- ~1800 gamma-ray emitting AGNs discovered
- 98% blazars, 2% nearby radio galaxies
- 30% FSRQs, 40% BL Lacs (45% HSPs) , 30% BCUs
- FSRQs redshifts up to 3.1, BL Lacs z<1
- FSRQs spectra are soft, BLLacs spectra are harder (pointing to different maximum energies reached by the emitting particles)
- Some gamma-ray spectra (mostly FSRQs) are curved: intrinsic, attenuation or superposition effect?
- Variability: strong in FSRQs, weaker in HSP BLLacs, sub-hour variability observed
- Location of dissipation region:
  - close to BH: short time scales, External Compton component
  - Far from BH: FSRQs detected at TeV, some radio flares simultaneous to GeV flares